

**Studies on enzymatic synthesis of optically active amides
for pharmaceutical intermediates**

Masutoshi Nojiri

2018

Contents

ABBREVIATIONS 2
INTRODUCTION 3
CHAPTER I	
Efficient asymmetric hydrolysis of 3-substituted glutaric acid diamides for gamma-aminobutyric acid (GABA) analog synthesis with an amidase 5
CHAPTER II	
Imidase catalyzing desymmetric imide hydrolysis forming optically active 3-substituted glutaric acid monoamides for gamma-aminobutyric acid (GABA) analog synthesis 32
CHAPTER III	
Characterization and application of an enantioselective amidase from <i>Cupriavidus</i> sp. 56
CONCLUSIONS 78
REFERENCES 80
ACKNOWLEDGEMENTS 85
PUBLICATIONS 86

ABBREVIATIONS

DNA	Deoxyribonucleic acid
HPLC	High-performance liquid chromatography
OD	Optical density
PCR	Polymerase chain reaction
rRNA	Ribosomal ribonucleic acid

INTRODUCTION

Chiral compounds play an important role in pharmaceutical development and manufacturing. Strategies used in asymmetric synthesis to produce single-enantiomer drugs provide important tools for pharmaceutical chemists. Over the past decades, biocatalysis has been established as a practical and environmentally friendly alternative to traditional catalysis both in the laboratory and on an industrial scale [1]. The numerous biocatalytic routes, scaled up for pharmaceutical manufacturing, demonstrate their competitiveness with traditional chemical processes [1]. Pure chiral amines, especially (*R*)-amines, are crucial building blocks in the synthesis of certain pharmaceutical drugs, such as Januvia[®] (sitagliptin), a drug for the treatment of type 2 diabetes [2]. Amine transaminases have been a focus of increased attention because of their ability to synthesize pure chiral amines, which are promising biocatalysts [2]. Amine transaminases transfer an amino group of a chiral amine compound to a ketone compound. However, depending on the targeted amine, there are instances when it is not possible to use a carbonyl compound as the raw material. Moreover, owing to the lower stability of carbonyl compounds, especially on an industrial scale, it is not always possible to use amine transaminases. Thus, the preparation of optically active amides using amidases (in combination with the Hofmann rearrangement), rather than amine transaminases, has been the main topic of research to enable chemoenzymatic synthesis of various optically active amines. Enzymatic procedures, including kinetic resolution or desymmetrization, have been reported for the preparation of optically active amides [3, 4]. However, the yield and optical purity of products have been insufficient for industrial production.

In this paper, I describe the preparation of (*R*)-3-substituted glutaric acid monoamide for (*R*)- γ -aminobutyric acid (GABA) analog synthesis, (*R*)-3-piperidinecarboxamide for the synthesis of (*R*)-3-aminopiperidine, and (*S*)-2-ethyl-2-methyl-malonamic acid for (*R*)-isovaline synthesis.

Chapter I describes the isolation of microorganisms that catalyze (*R*)-selective 3-(4-chlorophenyl) glutaric acid diamide (CGD) hydrolysis to produce (*R*)-3-(4-chlorophenyl) glutaric acid monoamide (CGM), a useful synthetic intermediate for the GABA analog arbaclofen [5]. In addition, I describe the gene cloning and purification of an amidase (*CoAM*) from *Comamonas* sp. KNK3-7 and the heterologous expression of this enzyme in *Escherichia*

coli. Furthermore, I improved the efficiency of CGD hydrolysis by using protein-engineered CoAM.

Chapter II describes the screening of microorganisms for amidases capable of catalyzing (*R*)-selective 3-(4-chlorophenyl) glutarimide (CGI) hydrolysis to produce (*R*)-CGM. I identified an amidase, BpIH, in *Burkholderia phytofirmans* DSM 17436, capable of (*R*)-selectively hydrolyzing CGI. In addition, the genes encoding BpIH and a homologous amidase from *Alcaligenes faecalis* NBRC 13111 were isolated, expressed in *E. coli*, and characterized.

Chapter III describes the unique characteristics of the novel amidase CsAM from *Cupriavidus* sp. KNK-J915 with (*S*)-selective (*RS*)-3-piperidinecarboxamide (NPD)-hydrolyzing activity. CsAM could catalyze the kinetic resolution of (*RS*)-NPD to produce (*R*)-NPD, a valuable synthetic intermediate for (*R*)-3-aminopiperidine, a common intermediate in the synthesis of dipeptidyl peptidase-4 (DPP-4) inhibitors [6, 7], such as Nesina[®] (alogliptin) and Tradjenta[®] (linagliptin). Furthermore, I showed that CsAM could hydrolyze prochiral 2-ethyl-2-methyl-malonamide (EMM) with high (*S*)-stereoselectivity to produce (*S*)-2-ethyl-2-methyl-malonamic acid (EMA). I also demonstrated the successful synthesis of (*R*)-isovaline by the Hofmann rearrangement using the highly optically pure (*S*)-EMA prepared with CsAM. (*R*)-Isovaline has been reported to activate the metabotropic GABA_B receptor and to act as an analgesic amino acid, thus having potential applications in the drug development field [8].

CHAPTER I

Efficient asymmetric hydrolysis of 3-substituted glutaric acid diamides for gamma-aminobutyric acid (GABA) analog synthesis with an amidase

(*R*)-Baclofen, an (*R*)-3-(4-chlorophenyl) gamma-aminobutyric acid, is a selective gamma-aminobutyric acid (GABA)_B agonist currently under clinical development for the treatment of autism spectrum disorders and fragile X syndrome [9]. Its synthesis has attracted the attention of many synthetic organic process chemists and several studies have been performed with the aim of improving the efficiency of the process [10, 11]. Optically active 3-substituted glutaric acid monoamide with high optical purity can be converted to GABA by the Hofmann rearrangement [12, 13] and is, therefore, a valuable synthetic intermediate for GABA.

The following enzymatic processes for producing optically active 3-substituted glutaric acid monoamide are known: (i) the esterase process, in which one ester group of a 3-isobutyl or 3-(4-chlorophenyl) glutaric acid diester is asymmetrically hydrolyzed using an esterase, and the resulting optically active 3-substituted glutaric acid monoester is then amidated [13, 14]; (ii) the nitrile hydratase process, in which one nitrile group of a 3-substituted glutaronitrile is asymmetrically hydrolyzed using enantioselective nitrile hydratase and a nonselective amidase, and the nitrile group of the resulting mononitrile-monocarboxylic acid is then hydrolyzed using an acid [15]. However, processes (i) or (ii) are not advantageous to industrial production in terms of yield and product optical purity.

Here my aim was to develop a novel biocatalytic process for obtaining an optically active 3-substituted glutaric acid monoamide by a microorganism or an enzyme capable of asymmetrically hydrolyzing 3-substituted glutaric acid diamide in a stereoselective manner.

In this study, a number of microorganisms were isolated which could catalyze (*R*)-selective 3-(4-chlorophenyl) glutaric acid diamide (CGD) and 3-isobutyl glutaric acid diamide (IBD) hydrolysis; thus, this enzymatic hydrolysis could be used to produce (*R*)-3-(4-chlorophenyl) glutaric acid monoamide (CGM) and (*R*)-3-isobutyl glutaric acid monoamide (IBM), useful synthetic intermediates for (*R*)-baclofen and pregabalin [Lyrica[®]; (*S*)-3-isobutyl GABA], respectively (Fig. 1-1). In addition, I describe the purification and gene cloning of an amidase—referred to as *CoAM*, from *Comamonas* sp. KNK3-7—and the

heterologous expression of *CoAM* in *Escherichia coli*, allowing further examination of the (*R*)-selective hydrolytic activity of *CoAM* on both CGD and IBD. Furthermore, I sought to improve the efficiency of *CoAM*-catalyzed CGD hydrolysis through mutation of individual amino acids thought to be involved in substrate binding.

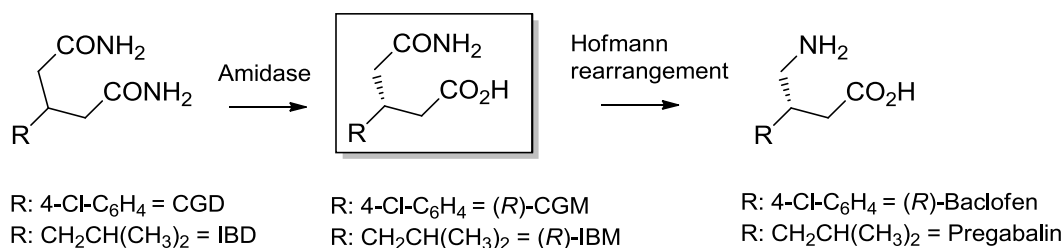


Figure 1-1. Synthesis of the intermediates of (*R*)-baclofen and pregabalin.

MATERIALS AND METHODS

Chemical reagents

CGD, (*R*)-CGM, IBD, (*RS*)-IBM and (*R*)-IBM were prepared as described below. (*RS*)-CGM was purchased from Wako Pure Chemicals Industries, Ltd. (Osaka, Japan). 3-(4-Chlorophenyl) glutaric acid (CGA) and 3-isobutyl glutaric acid (IBA) were purchased from Shanghai Richem International Co., Ltd (Shanghai, China). All other chemicals used in this study were of analytical grade and were commercially available.

Preparation of CGD and (*R*)-CGM

3-(4-Chlorophenyl) glutaric acid (CGA; 10.0 g; 41.2 mmol) was dissolved in methanol (60 ml), and thionyl chloride (12.3 g; 103 mmol) was added dropwise. After the addition, the resultant mixture was stirred for 2 h followed by distillation of the solvent at reduced pressure. Thus, a white solid of 3-(4-chlorophenyl) glutaric acid dimethyl (11.1 g; 41.2 mmol) was obtained. Solid 3-(4-chlorophenyl) glutaric acid dimethyl (8.0 g; 30.0 mmol) was placed in a pressure-proof container. An ammonia/methanol solution (wet weight: 80 g; 800 mmol) was then added. The container was then heated in a hermetically sealed system at 80°C and stirred for 3 days. Thereafter, the contents of the container were subjected to crude concentration to form a solid precipitate, which was collected by filtration. The filtered solid matter was dried at

reduced pressure to yield CGD (6.5 g; 27.0 mmol) as a white solid: $^1\text{H-NMR}$ (DMSO- d_6) δ (ppm): 2.28–2.49 (4H, m), 3.45 (1H, m), 6.66 (4H, brs), 7.19–7.50 (4H, m). (*R*)-CGM was prepared from (*RS*)-CGM following a procedure previously reported [12].

Preparation of IBD, (*RS*)-IBM and (*R*)-IBM

3-Isobutyl glutaric acid (IBA; 8.0 g, 42.5 mmol) was dissolved in methanol (50 ml), and thionyl chloride (13.7 g; 115 mmol) was added dropwise. After the addition, the resultant mixture was stirred for 2 h followed by distillation of the solvent at reduced pressure. Thus, an oily matter of 3-isobutyl glutaric acid dimethyl (9.3 g; 43.0 mmol) was obtained. The oily matter of 3-isobutyl glutaric acid dimethyl (9.0 g; 41.6 mmol) was placed in a pressure-proof container. An ammonia/methanol solution (wet weight: 90 g; 900 mmol) was then added. The container was then heated in a hermetically sealed system at 80°C and stirred for 5 days. Thereafter, the content of the container was subjected to crude concentration. The resulting solid precipitate was collected by filtration and dried at reduced pressure to yield IBD (2.3 g; 12.3 mmol): $^1\text{H-NMR}$ (DMSO- d_6) δ (ppm): 7.27 (2H, s), 6.71 (2H, s), 2.19 (1H, m), 2.00 (4H, d, $J = 6.0$ Hz), 1.62 (1H, m), 1.08 (2H, m), 0.82 (6H, d, $J = 6.0$ Hz). (*RS*)-IBM and (*R*)-IBM were prepared from IBA following a procedure previously reported [14].

Collection of CGD-assimilating microorganisms

Small soil samples collected from various places were each suspended in 5 ml physiological saline. The supernatant from each suspension (100 μl) was transferred to a separate test tube (21 \times 195 mm) containing 8 ml liquid isolation medium [0.5% (w/v) glycerol, 0.1% (w/v) K_2HPO_4 , 0.1% (w/v) KH_2PO_4 , 0.05% (w/v) $\text{MgSO}_4 \cdot 7\text{H}_2\text{O}$, 0.005% (w/v) $\text{ZnSO}_4 \cdot 7\text{H}_2\text{O}$, 0.003% (w/v) $\text{FeSO}_4 \cdot 7\text{H}_2\text{O}$, 0.0002% (w/v) $\text{CuSO}_4 \cdot 5\text{H}_2\text{O}$, 0.0005% (w/v) $\text{MnSO}_4 \cdot 4\text{H}_2\text{O}$, 0.001% (w/v) $\text{CoSO}_4 \cdot 7\text{H}_2\text{O}$, 0.1% (w/v) NaCl, 0.00002% (w/v) thiamine hydrochloride, 0.00002% (w/v) pyridoxine hydrochloride, 0.00002% (w/v) nicotinic acid, 0.00002% (w/v) pantothenic acid, 0.00002% (w/v) 4-aminobenzoic acid, 0.00002% (w/v) riboflavin, 0.000002% (w/v) biotin, 0.05% (w/v) cyclohexanecarboxamide and 0.15% (w/v) CGD (pH 7.0)] and incubated at 30°C with reciprocal shaking (300 rpm) for 5–6 days. Samples (100 μl) of the medium from tubes where microbial growth was observed were transferred to fresh test tubes (21 \times 195 mm) containing the same medium for further growth at 30°C with

reciprocal shaking for an additional 5–6 days. During this growth, aliquots of the media were withdrawn and the supernatants obtained on centrifugation (13000 g, 2 min) were analyzed as described below. The culture media, in which the production of (*R*)-CGM was observed, were selected, streaked onto agar plates with the same composition as the isolation medium supplemented with 1.5% (w/v) agar and grown at 30°C for 2–3 days. The colonies that appeared after growth were isolated as CGD-assimilating microorganisms and used for the following experiments.

Screening methods

Medium A comprised 2% (w/v) glycerol, 1% (w/v) meat extract, 1% (w/v) polypepton, 0.5% (w/v) yeast extract, 0.1% (w/v) K₂HPO₄ and 0.1% (w/v) KH₂PO₄ (pH 7.0). Medium B comprised Medium A supplemented with 0.1% (w/v) cyclohexanecarboxamide (pH 7.0). Medium C comprised Medium A supplemented with 0.1% (w/v) CGD (pH 7.0). Medium D comprised Medium A supplemented with 0.1% (w/v) glutaronitrile (pH 7.0). Each CGD-assimilating microorganism was inoculated in a test tube (21 × 195 mm) containing 8 ml Medium A, B, C or D and then cultivated at 30°C with reciprocal shaking (300 rpm) for 1–2 days. At this point, the microbial cells were harvested via centrifugation and resuspended in 2 ml 100 mM potassium phosphate buffer (pH 7.0). The resulting cell suspensions (1 ml each) were separately mixed with 1 mg CGD (4.15 mM) synthesized by the method described above, and the reaction mixtures were stirred at 30°C for 24 h. After the end of the reaction, aliquots of the reaction mixtures were withdrawn and analyzed by HPLC to determine the conversion rate (%) of the substrate to the product in the reaction solution and the optical purity (% *e.e.*) as described below.

Substrate specificity

Each of the selected strains was inoculated into a test tube (21 × 195 mm) containing 8 ml Medium B and then grown at 30°C with reciprocal shaking (300 rpm) for 1–2 days. At the end of the culture period, microbial cells were harvested via centrifugation and resuspended in 2 ml 100 mM potassium phosphate buffer (pH 7.0). The resulting cell suspensions (1 ml each) were separately mixed with 1 mg CGD (5.4 mM), and each of the reaction mixtures was stirred at 30°C for 20 h. After the end of the reaction, aliquots of the reaction mixtures were withdrawn

and analyzed by HPLC to determine the conversion rate (%) of the substrate to the product in the reaction solution and the optical purity (% *e.e.*) as described below.

Analytical methods

¹H-NMR spectra were recorded in DMSO-*d*₆ using a JM-400 FT-NMR spectrometer (400 MHz; Jeol, Japan). Chemical shifts are expressed in parts/million (ppm), with tetramethylsilane as the internal standard.

The degree of conversion of CGD to CGM was analyzed by reversed-phase HPLC using a Shimadzu LC-VP system (Shimadzu, Japan) equipped with a Cosmosil 5C₁₈-AR-II column (4.6 mm × 250 mm; Nacalai Tesque, Japan). HPLC was performed using acetonitrile:water (3:7, v/v; pH 2.5, adjusted with phosphoric acid) as the mobile phase, a flow rate of 0.7 ml/min, a column temperature of 35°C, and ultraviolet (UV) detection at 210 nm. The retention times of CGD and CGM were 7.3 and 10.8 min, respectively. The optical purity of CGM was determined by reversed-phase HPLC using a Shimadzu LC-VP system equipped with two Sumichiral OA-7000 columns (4.6 mm × 250 mm; Sumika Chemical Analysis Service Ltd, Japan). HPLC was performed using acetonitrile:water (2:8, v/v; pH 2.5, adjusted with phosphoric acid) as the mobile phase, a flow rate of 0.5 ml/min, a column temperature of 30°C, and UV detection at 210 nm. The retention times of (*S*)-CGM, (*R*)-CGM, and CGD were 33, 35.1, and 38.4 min, respectively. The degree of conversion of IBD to IBM was analyzed by reversed-phase HPLC using a Shimadzu LC-VP system (Shimadzu, Japan) equipped with a Cosmosil 5C₁₈-AR-II column (4.6 mm × 250 mm). HPLC was conducted using acetonitrile:water (2:8, v/v; pH 2.5, adjusted with phosphoric acid) as the mobile phase, a flow rate of 1.0 ml/min, a column temperature of 30°C, and UV detection at 210 nm. The retention times of IBD and IBM were 4.5 and 7.4 min, respectively. To determine the optical purity of IBM, IBM in the reaction solution was derivatized using phenacyl bromide and the derivatives were analyzed. The derivatization procedure was as follows: K₂CO₃ (30 mg), acetonitrile (400 mg), and phenacyl bromide (10 mg) were added to the reaction mixture (100 mg), which was stirred for 15 min. The mixture was separated by thin-layer chromatography (Merck, Darmstadt, Germany) (hexane:acetone 3:1, v/v, R_f 0.08) and the derivatives were extracted using ethyl acetate. The solution was concentrated under reduced pressure to remove ethyl acetate, and the residue was dissolved in water. The diluted solution was used as IBD derivatives. Determination

of the optical purity of IBM derivatives was performed by reversed-phase HPLC using a Shimadzu LC-VP system equipped with a Chiralpack AD-RH column (4.6 mm × 150 mm; Daicel Corporation, Japan). HPLC was performed using acetonitrile:water (1:1, v/v; pH 2.5, adjusted with phosphoric acid) as the mobile phase, a flow rate of 0.5 ml/min, a column temperature of 30°C, and UV detection at 210 nm. The retention times of (*S*)-IBM and (*R*)-IBM were 12.7 and 14.6 min, respectively.

Purification of CoAM from *Comamonas* sp. KNK3-7

Comamonas sp. KNK3-7 (NITE BP-963) was subcultured at 30°C for 7 h in a test tube containing 8 ml of basal medium (2% (w/v) glycerol, 1% (w/v) meat extract (Wako Pure Chemical Industries, Osaka, Japan), 1% (w/v) polypeptone (Wako), 0.5% (w/v) yeast extract (Wako), 1% (w/v) cyclohexanecarboxamide as an enzyme inducer, 0.1% (w/v) K₂HPO₄, 0.1% (w/v) KH₂PO₄, 0.05% (w/v) MgSO₄, 0.1% (w/v) NaCl, 0.0005% (w/v) FeSO₄·7H₂O, and 0.0005 % (w/v) CoSO₄·7H₂O (pH 7.0)). The subculture (0.3 ml) was inoculated into a 500-ml Sakaguchi flask containing 60 ml of basal medium. After 17 h of incubation at 30°C with reciprocal shaking (130 rpm), the subculture (15 ml) was then inoculated into a 5-L jar fermenter containing 3 L of basal medium. After 24 h of cultivation at 30°C (agitation rate 350 rpm, aeration rate 0.3 vvm), the cells were collected by centrifugation from 5 L of the cultured broth (from two jar fermenters), washed with 1 L of 20 mM potassium phosphate (pH 7.0), and suspended in 310 ml of 20 mM potassium phosphate containing 10% (w/v) glycerol (pH 7.0). All purification procedures were performed at 4°C. After ultrasonic disruption of the cells with an ultrasonic homogenizer (UH-600S; SMT Co., Ltd., Tokyo, Japan) for 90 min (pulse 50%, output 9, 1 min × 25), 450 ml of cell-free extract was obtained by centrifugation. Three grams of protamine sulfate and 110 ml of 20 mM potassium phosphate were added to the cell-free extract and the mixture was stirred for 30 min. The precipitate was discarded after centrifugation. The enzyme solution (490 ml) was applied to a 400-ml Toyopearl DEAE-650M column (Tosoh, Tokyo, Japan) equilibrated with 20 mM potassium phosphate containing 10% (w/v) glycerol (pH 7.0). The enzyme was eluted with a 0–0.3 M NaCl linear gradient. A total of 150 ml of enzyme solution was collected from the active fractions. Ammonium sulfate was added to the enzyme solution at a final concentration of 0.5 M. The enzyme solution (150 ml) was applied to a 120-ml Toyopearl Butyl-650S column (Tosoh) equilibrated with 20 mM potassium phosphate

(pH 7.0) containing 10% (w/v) glycerol and 0.5 M ammonium sulfate. The enzyme was eluted with a 0–0.5 M ammonium sulfate linear gradient. A total of 72 ml of enzyme solution was collected from the active fractions and dialyzed against 20 mM potassium phosphate containing 10% (w/v) glycerol (pH 7.0). The dialyzed enzyme solution (72 ml) was applied to a 6-ml Resource Q column (GE Healthcare Bio-Sciences) equilibrated with 20 mM potassium phosphate containing 10% (w/v) glycerol (pH 7.0). The enzyme was eluted with a 0–0.3 M NaCl linear gradient. A total of 1.9 ml of the enzyme solution was collected from the active fractions and dialyzed against 20 mM potassium phosphate containing 10% (w/v) glycerol (pH 7.0). The dialyzed enzyme solution (2 ml) was applied to a 4.5-ml Bio-Gel HT hydroxyapatite column (Bio-Rad Laboratories K.K., Tokyo, Japan) equilibrated with 1 mM potassium phosphate containing 10% (w/v) glycerol (pH 7.0). The enzyme was eluted with a 1–30 mM potassium phosphate linear gradient. A total of 1 ml of the enzyme solution was collected from the active fractions. The enzyme solution (1 ml) was applied to a 24-ml Superdex 200 HR 10/30 column (GE Healthcare Bio-Sciences) equilibrated with 20 mM potassium phosphate containing 10% (w/v) glycerol and 0.15 M NaCl (pH 7.0). The enzyme was eluted with 20 mM potassium phosphate containing 10% (w/v) glycerol and 0.15 M NaCl (pH 7.0). A total of 1 ml of the enzyme solution was collected from the active fractions and dialyzed against 20 mM potassium phosphate containing 10% (w/v) glycerol (pH 7.0). The active fractions were pooled and used as the purified enzyme.

Enzyme assay

Enzyme activity was monitored at each step during the purification of *CoAM* using an enzyme assay with CGD as a substrate. The standard reaction mixture (0.5 ml) contained 100 mM potassium phosphate buffer (pH 7.0), 8.3 mM CGD, and an appropriate amount of the enzyme. After incubation at 30°C for 0.5–2 h, the amount of CGM produced was determined using HPLC. One unit of activity was defined as the amount of enzyme catalyzing the formation of 1 μ mol of CGM per minute under the aforementioned conditions. Protein content was determined using the Quick StartTM Bradford Dye Reagent (Bio-Rad).

Determination of enzyme molecular weight

The molecular weight of the enzyme was estimated by sodium dodecyl

sulfate-polyacrylamide gel electrophoresis (SDS-PAGE) (10%) using Perfect Protein™ Markers (EMD Millipore, Billerica, MA, USA) as the standard.

Partial amino acid sequence determination

CoAM was separated from other peptides by HPLC on a YMC-Pack Protein-RP column (4.6 × 250 mm; YMC, Kyoto, Japan) equilibrated with 0.1% (w/v) trifluoroacetic acid and eluted with a linear acetonitrile gradient (10%–70%) at a flow rate of 1.0 ml/min. The HPLC-purified *CoAM* was digested with V8 protease (Wako) in 4 M urea and 100 mM NH₄HCO₃ buffer (pH 7.8) for 16 h at 30°C. The peptides were separated by HPLC as described above. The sequence was analyzed with a model 477A gas-liquid-phase protein sequencer (Applied Biosystems, Carlsbad, CA, USA).

Cloning of *CoAM* from *Comamonas* sp. KNK3-7

Genomic DNA from *Comamonas* sp. KNK3-7 was prepared using the GNOME® DNA isolation kit (MP Biomedicals, Santa Ana, CA, USA). The pUCT plasmid vector was obtained by eliminating the *NdeI* recognition sequence (CATATG was changed to CATATT by mutagenesis) of pUCNT, which was prepared from pUC19 and pTrc99A as described previously [16]. *E. coli* HB101 harboring plasmid vector, cultured at 30°C in 2-YT medium containing 1.6% (w/v) Bacto™ tryptone, 1% (w/v) Bacto™ yeast extract, and 0.5% (w/v) NaCl (pH 7.0) in the presence of ampicillin (0.1 mg/ml), was used for gene manipulations. Plasmid DNA was purified from *E. coli* using a QIAprep Spin miniprep kit (Qiagen, Hilden, Germany). DNA fragments were recovered from agarose gels using a QIAquick gel extraction kit (Qiagen). Restriction enzymes, a DNA ligation kit, T4 DNA ligase, Ex Taq DNA polymerase, and PrimeSTAR HS DNA polymerase for polymerase chain reaction (PCR) were purchased from Takara Bio (Shiga, Japan).

PCR amplification of the core region of the *CoAM* gene

The core region of the *CoAM* gene was amplified from *Comamonas* sp. KNK3-7 chromosomal DNA (100 ng) using the primers *CoAM*-F (5'-ATGCARYTNACNCAYGARCA-3') and *CoAM*-C (5'-TTYTGNGCYTTNGCRTARTA-3') (100 pmol each). Reactions were performed in a 50- μ l volume with dNTPs (10 nmol each) and

2.5 U Taq DNA polymerase with the proprietary buffer. The reaction was performed for 40 cycles (10 s at 98°C, 55 s at 50°C, and 1 min at 72°C) using a program temperature control system (PC-701; ASTEC, Fukuoka, Japan). The amplified fragment was purified and ligated into the pT7Blue T-vector (Merck).

Inverse PCR to amplify the DNA sequences flanking the core region

Chromosomal DNA from *Comamonas* sp. KNK3-7 was digested with *Eco*RI for 18 h at 37°C. The digested DNA was circularized with T4 DNA ligase. Amplification of circularized DNA (25 ng) by inverse PCR was performed using the primers *Co*AM-iF (5'-ACCCCATCGGCTGCGAAGGCCTGACCATGC-3') and *Co*AM-iR (5'-GGGCGCCATTCACCTCAGTCCTGTAATACC-3') (50 pmol each) with 2.5 U Ex Taq DNA polymerase. The reaction was performed for 35 cycles (30 s at 94°C, 30 s at 55°C, and 3 min at 72°C). The amplified DNA fragment was ligated into the pT7Blue T-vector.

Nucleotide sequencing

The cloned DNA fragments were sequenced using the dideoxy chain termination method with a dye-terminator cycle-sequencing kit (Applied Biosystems) and an ABI 373A DNA sequencer (Applied Biosystems). Sequence data were analyzed using Genetyx-Win software (Genetyx, Tokyo, Japan). *Co*AM amino acid sequences were aligned with the BLAST similarity search program (<http://www.ncbi.nlm.nih.gov/BLAST/>).

***Co*AM expression plasmid construction**

An expression plasmid, pCT*Co*AM, containing the *Co*AM gene, the lac promoter, and a terminator inserted into pUC19, was constructed. An N-terminal DNA primer (5'-CGGAATTCTAAGGAGGTTACAATGGCCATTGTTCCGCCCTACC-3') with an *Eco*RI site at the 5' end and a C-terminal DNA primer (5'-GCAGAGCTCTTACAACGTCTTCCAGTCGAC-3') with a *Sac*I site added immediately after the termination codon were synthesized. The *Co*AM gene was amplified by PCR with the two aforementioned primers (10 pmol each) from genomic DNA (10 ng) of *Comamonas* sp. KNK3-7. Amplification by PCR was performed in a reaction mixture (50 µl) with 1.25 U of PrimeSTAR HS DNA polymerase in the proprietary buffer. The reaction was performed for 30

cycles (10 s at 98°C, 5 s at 60°C, and 1.5 min at 72°C). The resulting DNA fragment was digested with *EcoRI* and *SacI* and then inserted into the *EcoRI*–*SacI* sites of pUCT to yield the recombinant plasmid pCTCoAM, which was transformed into *E. coli* HB101.

Site-directed mutagenesis

Mutations were introduced into the pCTCoAM template DNA by PCR using the QuikChange Site-Directed Mutagenesis Kit (Agilent Technologies, Santa Clara, CA, USA) according to the manufacturer's instructions. The primers used for mutagenesis are listed in Table 1-1. Successful introduction of desired mutations was confirmed by DNA sequencing.

Bioconversion of CGD to (R)-CGM and of IBD to (R)-IBM

Each *E. coli* transformant producing CoAM or its mutants was inoculated into 5 ml of 2-YT medium in a test tube (24 mm i.d. × 200 mm) and incubated at 30°C with reciprocal shaking (300 rpm) for 24 h. Microorganisms were harvested by centrifugation, resuspended in 100 mM potassium phosphate (pH 7.0), and then normalized for OD₅₅₀ (optical density of 12 at 550 nm) to ensure that equivalent cell numbers were used in reaction analyses. The resulting cell suspensions (1 ml each) were mixed with CGD (20.8 mM or 166.2 mM) or IBD (107.4 mM), and the reaction mixtures were stirred at 30°C. Aliquots of the reaction mixtures were taken at various time points, and centrifuged. The supernatants were analyzed by HPLC to determine the degree of substrate conversion (%) and the optical purity (% *e.e.*).

Analysis of substrate affinities of recombinant CoAM and its mutants

Apparent K_m values for CGD were calculated from Hanes–Wolf plots generated on the basis of the results of the aforementioned standard activity assays with recombinant CoAM and its mutants (using cell-free extracts) and varying substrate concentrations.

Three-dimensional (3D) protein structure homology modeling of CoAM

3D protein structure homology modeling of CoAM complexed with CGD was performed using atomic coordinates determined by using the X-ray crystallographic structure of another amidase, RhAmidase, derived from *Rhodococcus* sp. N-771, complexed with benzamide (PDB ID code: 3A1I) as a template [17]. Insertions, deletions, and substitutions of

amino acid residues were modeled with Homology Modeling Professional for HyperChem (Molfunction, <http://www.molfunction.com/>). The 3D structure model of CGD was constructed using Chem3D (CambridgeSoft, <http://www.cambridgesoft.com/>). Selection of the preferable side-chain conformation of *CoAM*, including the L146A and L146M mutants, and energy minimization of the *CoAM*/CGD complex were performed using the same homology modeling program. Graphic representations of the RhAmidase/benzamide and *CoAM*/CGD complexes were generated with PyMOL (Schrödinger, <https://www.pymol.org/>).

Table 1-1 PCR primers used in site-directed mutagenesis.

Primer name	Nucleotide sequence (5'-3')
L146M-F	GCACTACTGCATGTCCGGTGGCAGC
L146M-R	GCTGCCACCGGACATGCA GTA GTGC
L146A-F	GCACTACTGCGCGTCCGGTGGCAGC
L146A-R	GCTGCCACCGGACGCGCA GTA GTGC
L146Q-F	GCACTACTGCCAGTCCGGTGGCAGC
L146Q-R	GCTGCCACCGGACTGGCA GTA GTGC
L146I-F	GCACTACTGCATTTCCGGTGGCAGC
L146I-R	GCTGCCACCGGAAA TGCAGTA GTGC
L146T-F	GCACTACTGCACCTCCGGTGGCAGC
L146T-R	GCTGCCACCGGAGGTGCA GTA GTGC
L146V-F	GCACTACTGCGTGTCCGGTGGCAGC
L146V-R	GCTGCCACCGGACA CGCA GTA GTGC
L146S-F	GCACTACTGCAGCTCCGGTGGCAGC
L146S-R	GCTGCCACCGGAGCTGCA GTA GTGC
L146G-F	GCACTACTGCGGCTCCGGTGGCAGC
L146G-R	GCTGCCACCGGAGCCGCA GTA GTGC
L146F-F	GCACTACTGCTTTTCCGGTGGCAGC
L146F-R	GCTGCCACCGGAAA AGCA GTA GTGC
L146N-F	GCACTACTGCAACTCCGGTGGCAGC
L146N-R	GCTGCCACCGGAGTTGCA GTA GTGC
L146H-F	GCACTACTGCCATTCCGGTGGCAGC
L146H-R	GCTGCCACCGGAA TGGCA GTA GTGC
L146Y-F	GCACTACTGCTATTCCGGTGGCAGC
L146Y-R	GCTGCCACCGGAA TAGCA GTA GTGC
L146K-F	GCACTACTGCAAA TCCGGTGGCAGC
L146K-R	GCTGCCACCGGATTTGCA GTA GTGC
L146C-F	GCACTACTGCTGCTCCGGTGGCAGC
L146C-R	GCTGCCACCGGAGCAGCA GTA GTGC
L146D-F	GCACTACTGCGATTCCGGTGGCAGC
L146D-R	GCTGCCACCGGAA TCGCA GTA GTGC
L146E-F	GCACTACTGCGAA TCCGGTGGCAGC
L146E-R	GCTGCCACCGGATTCGCA GTA GTGC
L146W-F	GCACTACTGCTGGTCCGGTGGCAGC
L146W-R	GCTGCCACCGGACCA GCA GTA GTGC
L146R-F	GCACTACTGCCGCTCCGGTGGCAGC
L146R-R	GCTGCCACCGGAGCGGCA GTA GTGC
L146P-F	GCACTACTGCCCGTCCGGTGGCAGC
L146P-R	GCTGCCACCGGACGGGCA GTA GTGC

RESULTS

Screening for (*R*)-selective CGD-hydrolyzing microorganisms

One hundred and twenty-two soil samples were tested to collect CGD-assimilating microorganisms. In the 15 culture media, the production of (*S*)-CGM with optical purity of over 90% *e.e.* was observed. On the other hand, in the 4 culture media, the production of (*R*)-CGM with optical purity of over 80% *e.e.* was observed, and four CGD-assimilating and (*R*)-CGM-producing bacterial strains were isolated. These strains were tested for their ability to hydrolyze CGD to optically active CGM (Table 1-2). All strains cultured in Medium B produced (*R*)-CGM. No CGA production was observed by any of the strains. These data indicated that the four strains have an amidase capable of hydrolyzing only CGD with (*R*)-selectivity.

Among the four strains, the highest optical purity (98.7% *e.e.*) was observed in the reaction with strain 3-7 and the lowest optical purity (94.4% *e.e.*) was observed in the reaction with strain 3-9 (Table 1-2). Strain 3-7 was selected as the most potent strain for CGD microbial hydrolysis because it gave the desired (*R*)-CGM with highest enantioselectivity from CGD, the corresponding diamide among the four strains.

Table 1-2 Isolated microorganisms producing (*R*)-CGM through CGD desymmetrization.

Strain	Medium for growth	CGM		CGA
		Conversion (%)	Stereoselectivity (% <i>e.e.</i>)	Conversion (%)
3-7	B	63.3	98.7 (<i>R</i>)	Not detected
3-9	B	31.2	94.4 (<i>R</i>)	Not detected
10-10	B	48.1	98.2 (<i>R</i>)	Not detected
24-9	B	73.8	98.4 (<i>R</i>)	Not detected

Effect of cyclohexanecarboxamide, CGD and glutaronitrile on enzyme induction

I examined the culture conditions of the four strains to identify those favorable for amidase production. These strains were cultured in Medium A, Medium B, Medium C or Medium D. All strains that were cultured in Medium A, C or D produced less CGM (0%–1.6% conversion). The addition of cyclohexanecarboxamide (Medium B) induced amidase activity.

Identification of strain 3-7

I conducted molecular phylogenetic analysis of strain 3-7 based on the nucleotide sequence of its 16S ribosomal DNA (rDNA). An initial BLAST search revealed that the nucleotide sequence of the 16S rDNA (accession No. AB821276, DDBJ/EMBL/GenBank databases) of strain 3-7 matched that of *Comamonas testosteroni* strain ATCC11996, with a homology of 99.9%. A homology search of GenBank/DDBJ/EMBL revealed that the 16S rDNA of strain 3-7 showed high homology with that of *C. testosteroni* KS0043. Furthermore, in a simplified molecular phylogenetic analysis using the 16S rDNA of strain 3-7 and the 16S rDNA of the 15 most homologous strains retrieved from the bacterial strain database, strain 3-7 was found to belong to the same phylogenetic branch as *C. testosteroni* ATCC11996, showing that they are very closely related (data not shown). Thus, the isolated strain 3-7 may belong to the genus *Comamonas*, probably to a group closely related to *C. testosteroni*. However, because it may not belong to *C. testosteroni*, it was named *Comamonas* sp. KNK3-7 and deposited as a collection number of NITE BP-963 in Nite Patent Microorganisms Depository (NPMD; <http://www.nbrc.nite.go.jp/npmd/e/>).

Microbial asymmetric IBD hydrolysis

Microbial IBD hydrolysis using washed cells of the selected four strains that were cultured in Medium B was followed (Table 1-3). After a 20-h reaction with 0.1% (w/v) IBD (5.4 mM) as the substrate and washed cells of *Comamonas* sp. KNK3-7 and strain 24-9 as the catalyst, (*R*)-IBM was formed with high optical purity >99.0% *e.e.* In contrast, IBD hydrolysis by strains 3-9 and 10-10 yielded (*R*)-IBM with lower optical purity (98.5% *e.e.* and 98.0% *e.e.*, respectively) than that produced by *Comamonas* sp. KNK3-7 and strain 24-9 as the catalyst. IBA production was not observed in any of the strains.

Table 1-3 Isolated microorganisms producing (*R*)-IBM through IBD desymmetrization.

Strain	Medium for growth	IBM		IBA
		Conversion (%)	Stereoselectivity (% <i>e.e.</i>)	Conversion (%)
3-7	B	59.4	>99 (<i>R</i>)	Not detected
3-9	B	60.6	98.5(<i>R</i>)	Not detected
10-10	B	41.9	98.0 (<i>R</i>)	Not detected
24-9	B	94.0	>99 (<i>R</i>)	Not detected

Purification of an (*R*)-selective CGD-hydrolyzing enzyme (*CoAM*)

CoAM was purified from a cell-free extract of cultured *Comamonas* sp. KNK3-7 cells by five-step column chromatography. *CoAM* catalyzed the hydrolysis of CGD with (*R*)-selectivity, producing CGM (98.8% *e.e.*). The purified enzyme migrated as a single band with an apparent molecular weight (M_r) of 54,000 on a 10% polyacrylamide gel (Fig. 1-2). The specific activity of *CoAM* prior to the first column chromatographic step was 0.13 mU/mg. After the third step, the yield was <3% and the specific activity was 14.3 mU/mg. The total and specific activity of *CoAM* decreased rapidly after the fourth chromatographic step due to its instability.

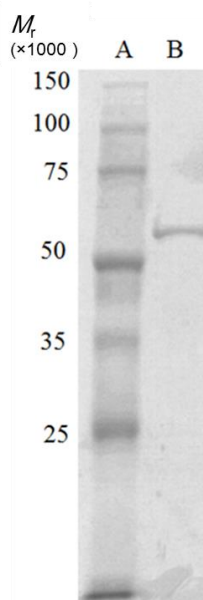


Figure 1-2. SDS-PAGE analysis of *CoAM* from *Comamonas* sp. KNK3-7. (A) Perfect Protein™ Markers, molecular weight 15,000-150,000, (B) purified enzyme.

Partial amino acid sequence of *CoAM*

The N-terminal amino acid sequence of *CoAM* was determined as MAKVRPTLDQLQDKAGRLNMQLTHEQAAEYL by peptide sequencing. One internal peptide was successfully separated by reverse-phase HPLC and its amino acid sequence was determined as GFQLANQDPRVADKVR SALARL. The N-terminal amino acid sequence of *CoAM* was BLAST searched against the NCBI nr protein sequence database and was found to be identical to an amidase from *Pseudomonas chlororaphis* B23 (GenBank: BAA14244) and an amidase from *Pseudomonas* sp. K-9 (GenBank: BAD98531).

Cloning and nucleotide sequence of the *CoAM* gene

Based on the N-terminal amino acid sequences and the conserved amino acid sequences of the aforementioned amidases identified by using BLAST, primers *CoAM*-F and *CoAM*-R were synthesized to amplify the core region (1032 bp) of the *CoAM* gene. The PCR product was cloned into the pT7Blue T-vector and sequenced. To clone the 5'- and 3'-flanking regions of the core region, self-circularized DNA of *EcoRI*-digested chromosomal DNA was used as a template for inverse PCR. Based on the nucleotide sequence of the core region, primers *CoAM*-iF and *CoAM*-iR were synthesized to amplify the 5'- and 3'-flanking regions. The PCR product was cloned into the pT7Blue T-vector and sequenced. The nucleotide sequences of the 5'- and 3'-flanking regions and core region were connected and the initiation (ATG) and termination (TGA) codons were identified. The *CoAM* gene data were deposited in the DDBJ DNA database under accession number LC015664. The sequence consisted of one open reading frame (1512 bp, 504 amino acids), and the deduced amino acid sequence contained regions identical to the partial amino acid sequence found by peptide sequencing except for two lysine residues in the N-terminal sequence. The predicted molecular weight of 54,054 corresponded precisely with the molecular weight of 54,000 estimated by SDS-PAGE analysis.

Amino acid sequence of *CoAM*

The deduced amino acid sequence of *CoAM* was compared with other protein sequences using BLAST. *CoAM* showed a high degree of identity with an amidase from each of the following: *P. chlororaphis* B23 (87%; GenBank: BAA14244), *Pseudomonas* sp. K-9 (85%;

GenBank: BAD98531), *Klebsiella pneumoniae* 342 (75%; GenBank: ACI08075), and *Rhodococcus* sp. N-771 (49%; GenBank: BAA36596).

CoAM-catalyzed asymmetric hydrolysis of CGD

The production of (*R*)-CGM from CGD by *CoAM*-transformed *E. coli* was investigated and the effect of the substrate concentration on asymmetric hydrolysis was examined. As shown in Fig. 1-3, all the CGD in the low-concentration (21 mM) reaction mixture was consumed after 3 h, and the optical purity of the produced (*R*)-CGM was 98.8% *e.e.*. In contrast, in the high-concentration (166 mM) CGD hydrolysis reaction, the substrate was not completely consumed even after 28 h. The reaction speed gradually decreased after 3 h, and no further CGD hydrolysis was detectable after 25 h, possibly due to inhibition of the hydrolysis reaction by the product, (*R*)-CGM.

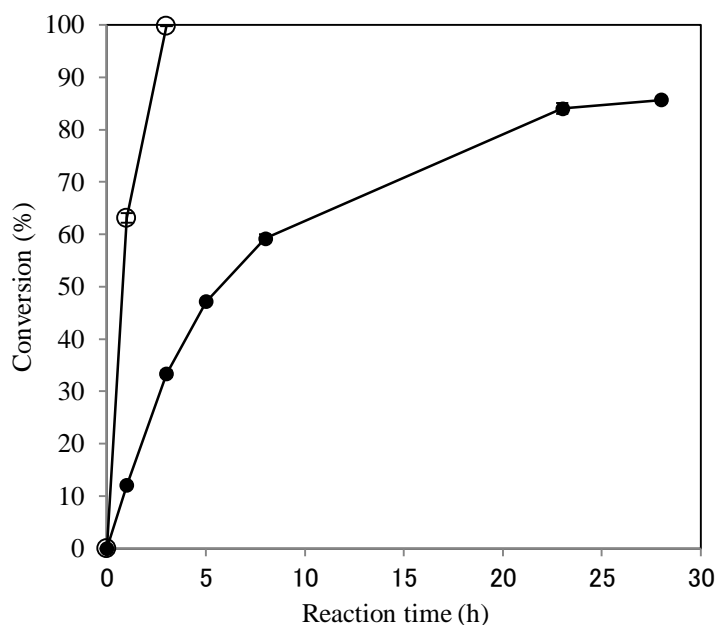


Figure 1-3. Time course of asymmetric hydrolysis of CGD by *CoAM*. The conversion of CGD (21 mM or 166 mM) to CGM by *CoAM*-transformed *E. coli* was monitored over a time course by reversed-phase HPLC. Filled circles, 166 mM CGD; open circles, 21 mM CGD. Values indicate means of results and SEs of results from three independent experiments.

Strategy to improve the reactivity of *CoAM* based on the catalytic residues of the *RhAmidase* from *Rhodococcus* sp. N-771

In *RhAmidase*, a number of amino acids, including Ser171, Ser195, and Lys96, have been shown to be essential for substrate hydrolysis [17]. The active site is surrounded by the hydrophobic residues Phe146, Ile227, Trp328, Leu447, and Ile450, indicating that it is narrow and hydrophobic [17]. As shown in Fig. 1-4, *CoAM* shares amino acid identity across this site with the exception of residue 146. It has been reported that Phe146 of *RhAmidase* may change its side chain conformation to recognize the substrate, depending on the size or shape of the substrate [17]. Accordingly, I generated 19 mutants, replacing Leu146 of *CoAM* with other amino acids, to determine if these mutants could improve the efficiency of hydrolysis in the 166 mM CGD reaction.

```

CoAM from C. sp. NITE BP-963 1:MAIVRPTLDQLQDIAGRLNMQLTHEQAAYLALMQPSFDAYDLVDELPDFTPPVRYDRSS 60
RhAmidase from R. sp. N-771 1:MATIRPDDKAIIDAAARHYGITLTKARLEWLPALIDGALGSYDVVDQLYADEATPPPTSRE 60
      ** * * * * *
CoAM from C. sp. NITE BP-963 61:GYRPSNPQNLLNAWYRYRTEVNGAREGKLAGKTVALKDNISLAGVPMNGATPLEGFVPKF 120
RhAmidase from R. sp. N-771 61:HAVPSASENPLSAWYVTTSSIPPTSDGVLTRRVAIKDNVTVAGVPMNGSRTVEGFTPSR 120
      * * * * * * * * * * * * * * * * * * * * * * * * * * * * * * * * * * * * * * * * *
CoAM from C. sp. NITE BP-963 121:DATVVTLLDAGATILGKATCEHYCFSSGGSHTSDPAPVHNPNYRHGFAAGGSSSGSAAALVA 180
RhAmidase from R. sp. N-771 121:DATVVTLLAAGATVAGKAVCEDLCSSGSSFTPASGPVVRNPWDRQREAGGSSSGSAAALVA 180
      * * * * * * * * * * * * * * * * * * * * * * * * * * * * * * * * * * * * * * * * *
CoAM from C. sp. NITE BP-963 181:AGEVDLAVGGDQGGSIIRIPSAFCGTYGMKPTHGLVPYTGIMAIEATIDHAGPIITRNVRDN 240
RhAmidase from R. sp. N-771 181:NGDVFDAIGGDQGGSIIRIPAAFCGVVGHKPTFGLVVPYTGAFPIERTIDHGLPIITRVHDA 240
      * * * * * * * * * * * * * * * * * * * * * * * * * * * * * * * * * * * * * * * * *
CoAM from C. sp. NITE BP-963 241:ALMLEVMAGADGLDPRQAAPQVDAYCDYLERGVSGLRIGILQEGFQLANQDPRVADKVRSS 300
RhAmidase from R. sp. N-771 241:ALMLSVIAGRDNDRQADSVEAGDYLSTLDSVDGLRIGIVREGFGHVAVSQPEVDDAVR 300
      * * * * * * * * * * * * * * * * * * * * * * * * * * * * * * * * * * * * * * * * *
CoAM from C. sp. NITE BP-963 301:AIARLEVLGARVEEVSVPENHLAGSLWHPIGCEGLTMQMHGNGAGFNWKGLYDVGLLD 359
RhAmidase from R. sp. N-771 301:AAASHLTEIGCTVEEVNIPWHLHAFHINNVIAITDGGAYQLMDGNGYGMNAEGLYDPELMA 360
      * * * * * * * * * * * * * * * * * * * * * * * * * * * * * * * * * * * * * * * * *
CoAM from C. sp. NITE BP-963 360:KQAGWREQANALSASLKLKCMFVGQYGLERYNGRFYAKAQNARFARAGYDKALQTYDLLV 419
RhAmidase from R. sp. N-771 361:HFASRRIQHADALSETVKLVALTGHGGITTLGGASYGKARNLVPLARAAYDTALRQFDVL 420
      * * * * *
CoAM from C. sp. NITE BP-963 420:MPTVPPIAQPHPEPCDSITDYVARALEMIGNTAPQDITGHPPAMSIKGLVDGLPLGLMF 478
RhAmidase from R. sp. N-771 421:VMPTLPYVASELPAKDVRATFITKALSMIANTAPFDVTGHPSLSVPAGLVNGLPVGMMI 480
      * * * * * * * * * * * * * * * * * * * * * * * * * * * * * * * * * * * * * * * * *
CoAM from C. sp. NITE BP-963 479:VGKHYAEGTIYQAAAFAEAAVDWKTL 504
RhAmidase from R. sp. N-771 481:TGRHFDDATVLRVGRFAFEKLRGAFPTPAERASNSAPQLSPA 521
      * * * * *

```

Figure 1-4. Comparison of the deduced amino acid sequence of *CoAM* from *Comamonas* sp. KNK3-7 with that of *RhAmidase* from *Rhodococcus* sp. N-771. Gaps in the aligned sequences are indicated by dashes. Asterisks indicate highly conserved amino acid residues. The amino acid residues that compose the active substrate-binding site are inserted in boxes.

Asymmetric hydrolysis of CGD by *CoAM* mutants

The production of (*R*)-CGM from 166 mM CGD was investigated using equivalent numbers of 19 different mutant-producing recombinant *E. coli* cells. The results are shown in Table 1-4. The reactivity of mutants L146Q, L146I, L146T, L146V, and L146S was similar to that of wild-type *CoAM*, and the reactivity of mutants L146G, L146F, L146N, L146H, L146Y, L146K, and L146C was lower than that of wild-type *CoAM*. Cells expressing L146D, L146E, L146W, L146R, and L146P showed no CGD-hydrolyzing activity. As shown in Fig. 1-5, two mutants, L146M and L146A, were able to almost completely consume the CGD within 4 and 8 h, respectively, considerably faster than wild-type *CoAM*. The optical purity of (*R*)-CGM in both mutants was >99% *e.e.*, compared to 98.8% for the wild type. The productivity of *CoAM*, L146M, and L146A in *E. coli* cells was investigated by SDS-PAGE analysis (Fig. 1-6). They did not exhibit great differences in visual judgement. The K_m values of *CoAM*, L146M, and L146A for CGD are shown in Table 1-5. The three variants had greatly different affinities for CGD.

Table 1-4 Production of (*R*)-CGM through asymmetric hydrolysis by wild-type and mutant *CoAM*.

Enzyme	Reaction time (h)	Produced CGM	
		Conversion (%)	Stereoselectivity (% <i>e.e.</i>)
<i>CoAM</i>	23	84	98.8 (<i>R</i>)
L146M	4	99	>99 (<i>R</i>)
L146A	8	99	>99 (<i>R</i>)
L146Q	23	96	>99 (<i>R</i>)
L146I	23	90	>99 (<i>R</i>)
L146T	23	89	>99 (<i>R</i>)
L146V	23	86	>99 (<i>R</i>)
L146S	23	83	>99 (<i>R</i>)
L146G	23	28	98.1 (<i>R</i>)
L146F	23	19	97.8 (<i>R</i>)
L146N	23	19	>99 (<i>R</i>)
L146H	23	18	>99 (<i>R</i>)
L146Y	23	9	98.9 (<i>R</i>)
L146K	23	4	Not detected
L146C	23	2	Not detected
L146D	23	Not detected	Not detected
L146E	23	Not detected	Not detected
L146W	23	Not detected	Not detected
L146R	23	Not detected	Not detected
L146P	23	Not detected	Not detected

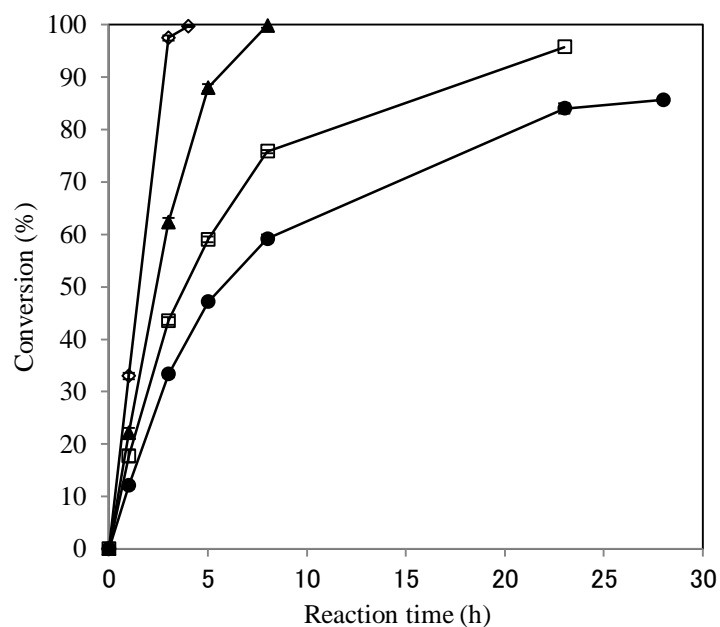


Figure 1-5. Time course of asymmetric hydrolysis of 166 mM CGD by *CoAM* mutants. The conversion of CGD (166 mM) to CGM by wild-type or mutant *CoAM*-transformed *E. coli* was monitored over a time course by reversed-phase HPLC. Filled circles, *CoAM*; open diamonds, L146M; filled triangles, L146A; and open squares, L146Q. Values indicate means of results and SEs of results from three independent experiments.

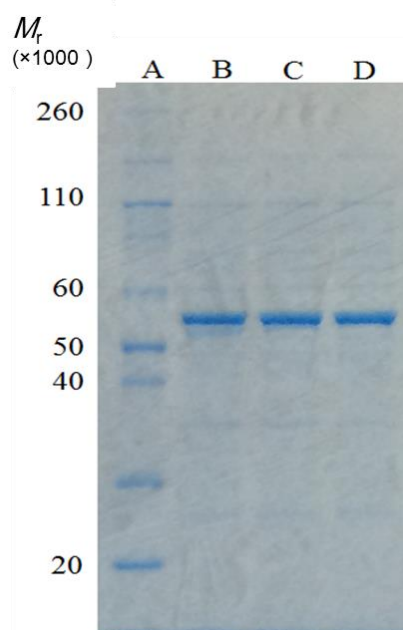


Figure 1-6. SDS-PAGE analysis of the cell-free extract of *E. coli* overexpressing *CoAM*, L146M, and L146A. The total amount of protein applied to each sample well was 1 μ g. (A) Novex® Sharp Unstained Protein Standards, molecular weight 3,500-260,000, (B) *CoAM*, (C) L146M, (D) L146A.

Table 1-5 Kinetic properties of recombinant *CoAM*, L146M, and L146A in CGD hydrolysis.

Enzyme	K_m (mM)
<i>CoAM</i>	10.0
L146M	1.2
L146A	6.3

CoAM- and mutant-catalyzed asymmetric hydrolysis of IBD

The production of (*R*)-IBM from 107 mM IBD was investigated using equivalent numbers of *CoAM*-, L146M-, and L146A-producing recombinant *E. coli* cells. As shown in Table 1-6, *CoAM*- and L146M-producing *E. coli* almost completely consumed IBD after 5 h, and the optical purity of the resulting (*R*)-IBM was 98.9% *e.e.*. In contrast, L146A-producing *E. coli* did not completely consume the substrate after 18 h and the optical purity of the resulting (*R*)-IBM was only 38.1% *e.e.*.

Table 1-6 Production of (*R*)-IBM through asymmetric hydrolysis by wild type and mutant *CoAM*.

Enzyme	Reaction time (h)	Produced IBM	
		Conversion (%)	Stereoselectivity (% <i>e.e.</i>)
<i>CoAM</i>	5	99	98.9 (<i>R</i>)
L146M	5	99	98.9 (<i>R</i>)
L146A	18	58	38.1 (<i>R</i>)

DISCUSSION

(*R*)-CGM is a useful chemical intermediate for the production of (*R*)-baclofen. Enantioselective enzymatic hydrolysis of CGD, the corresponding diamide, is one of the most effective strategies for its synthesis. Producing (*R*)-CGM with high optical purity requires an amidase showing high enantioselectivity.

I isolated four microorganisms that hydrolyzed CGD with (*R*)-selectivity from soil samples using a medium containing cyclohexanecarboxamide and CGD as the main nitrogen source. The CGD-assimilating microorganisms hydrolyzed CGD in various portions of enantiomers. The number of microorganisms that hydrolyzed CGD with (*S*)-selectivity was much more than the number of microorganisms with *R*-selectivity, but all four strains exhibited high (*R*)-selectivity. The strain KNK3-7, which was identified as *Comamonas* sp., was selected as the most promising strain because it produced (*R*)-CGM with the highest enantioselectivity. *Rhodococcus rhodochrous* J1 produced at least two amidases one of which seemed to be induced by cyclohexanecarboxamide [18]. These amidases produced by *R. rhodochrous* J1 were involved in nitrile metabolism, with a genetically linked nitrile hydratase [19]. The amidase from *C. testosterone* 5-MGAM-4D was also involved in nitrile metabolism, with a genetically linked nitrile hydratase [20, 21]. In contrast, the amidase from *C. acidovorans* KPO-2771-4 did not seem related to nitrile metabolism [22]. Amidase production from *Comamonas* sp. KNK3-7 was induced by cyclohexanecarboxamide. These data suggest that the amidase from *Comamonas* sp. KNK3-7 is involved in nitrile metabolism, with a genetically linked nitrile hydratase.

It has been reported that the asymmetric hydrolysis of 3-isobutyl glutaric acid diisopropyl ester carried out with porcine liver esterase yielded (*S*)-3-isobutyl glutaric acid monoester with an optical purity of 85% *e.e.* [14]. The resulting (*S*)-3-isobutyl glutaric acid monoester was converted to (*R*)-IBM with an optical purity that may be lower than our results. This indicates that the asymmetric hydrolysis of IBD using the amidase from *Comamonas* sp. KNK3-7 is a more efficient method to produce (*R*)-IBM with higher optical purity.

I purified an (*R*)-specific, CGD-hydrolyzing enzyme from *Comamonas* sp. KNK3-7 and verified that the enzyme (*CoAM*) hydrolyzes CGD in an (*R*)-selective manner. During the purification of *CoAM*, the enzyme activity rapidly decreased; therefore, I could not analyze its specific activity for CGD and further characterize the purified enzyme. I determined partial

amino acid sequences of the purified enzyme, which allowed me to clone and sequence the gene encoding the enzyme. The deduced amino acid sequence of *CoAM* shared the highest identity (87%) with an amidase from *P. chlororaphis* B23, a catalyst for the industrial production of acrylamide [23, 24]. Thus, the amidase from *P. chlororaphis* B23 and its homologs might be active towards 3-substituted glutaric acid diamides.

The hydrolytic activity of recombinant *CoAM* decreased with increasing concentration of CGD. The solubility of CGD in 100 mM potassium phosphate (pH 7.0) is approximately 4.2 mM, whereas the solubility of the product, CGM, is substantially greater (400 mM or more under the reaction conditions). Consequently, as the reaction progresses, the system turns from a slurry state into a solution. Thus, it is likely that in high-concentration reactions, *CoAM* is inhibited by the reaction products. Accordingly, I aimed to improve reactivity by creating a *CoAM* mutant having increased substrate affinity. In a comparison of the eight amino acids suggested to be important for enzyme activity based on a reported X-ray crystallographic structure of RhAmidase [17], I found that only amino acid 146 of *CoAM* differed from that of RhAmidase (Fig. 1-4). RhAmidase contains a phenylalanine at this position, which has been reported to play an important role in substrate recognition, whereas *CoAM* contains a leucine at position 146. Therefore, I investigated whether substitution of this amino acid by protein engineering would improve the enzyme reactivity. My results indicated that the methionine-substituted L146M and alanine-substituted L146A mutant enzymes exhibited increased reactivity, completing the reaction with 166 mM CGD in 4 and 8 h, respectively. Moreover, the mutations improved the stereoselectivity, with increased optical purity of (*R*)-CGM (to >99% *e.e.*) as compared with that obtained with wild-type *CoAM*. Kinetic analysis of *CoAM*, L146M, and L146A showed that the mutants had higher affinity for CGD than the wild-type enzyme, corroborating their improved affinity for CGD. In addition, the K_m value for L146M was 1.2 mM, which was lower than the solubility of CGD (4.2 mM) under the reaction conditions.

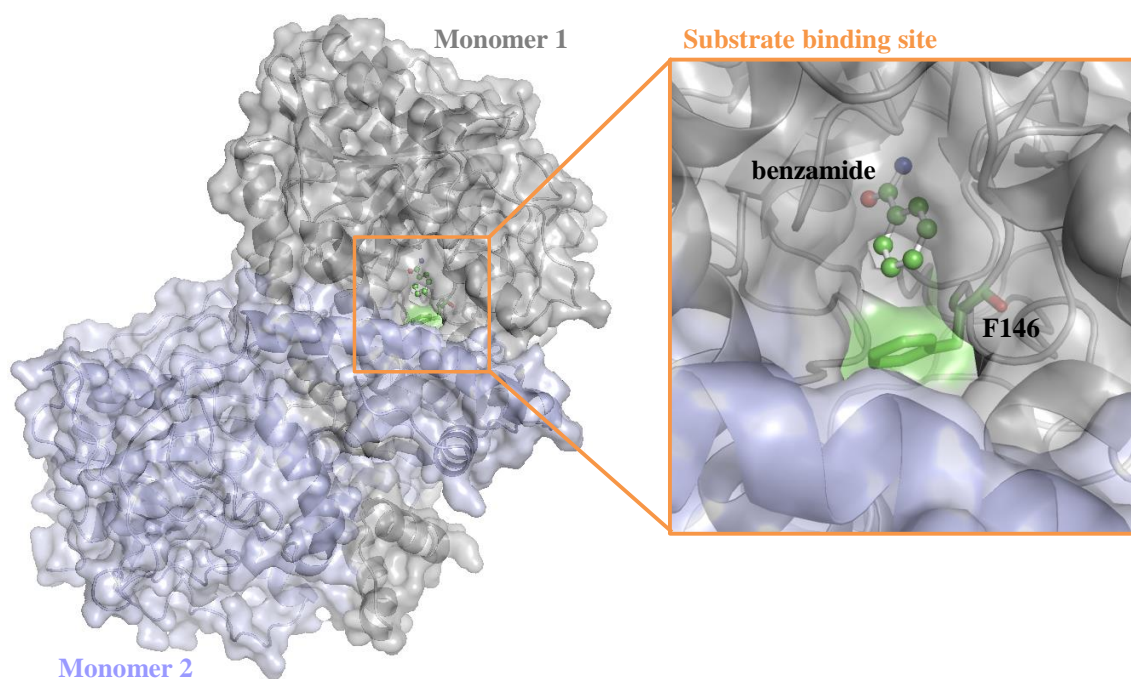
To understand how these amino acid substitutions might affect enzyme reactivity, I analyzed the structure of the substrate-binding pocket using RhAmidase [17] as a model. As shown in Fig. 1-4, Leu146 in *CoAM* corresponds with Phe146 in RhAmidase. Phe146 is located near a putative entrance to the substrate-binding pocket in the crystal structure of a RhAmidase/benzamide complex (Fig. 1-7). I predicted the 3D structure of the wild type, L146A,

and L146M *CoAM* complexed with CGD using homology modeling. The structural models were constructed under the assumption that *CoAM* is composed of two monomers and the relative position of the reactive amide group of CGD in the *CoAM*/CGD complex should be the same as that of benzamide in the RhAmidase/benzamide complex. In these structural models, residue 146 is also located near a cavity of the substrate-binding site and is close to another (nonreactive) amide group of CGD, as shown in Fig 1-7. By widening this cavity, the L146A mutant could promote turnover of the substrate. In the L146M/CGD complex model, the methionine sulfur atom is located close to the main-chain carbonyl oxygen atom of Ser374. It has been reported that there is a non-hydrogen bond interaction between the methionine sulfur atom and an oxygen atom of the main-chain carbonyl group [25]. This interaction might result in a widening of the cavity. If this conformation shift was to occur, the turnover of substrate may be further promoted. In contrast, substitution with other nonpolar (hydrophobic) amino acids having aromatic rings or β -branched side chains (e.g., Phe, Tyr, Trp, Ile, and Val) could result in a narrowing of the cavity and, therefore, reduced substrate turnover. Substitutions with polar amino acids may also impair enzymatic activity via the interaction between their polar groups and the amide group of CGD, also resulting in impaired substrate turnover.

When hydrolysis of IBD by the L146M and L146A mutants was monitored, L146M showed approximately the same activity and stereoselectivity as the wild type, whereas both of these properties were reduced for L146A. It is noteworthy that differences in the reactivity and stereoselectivity of the enzymes depended on whether the substitution site 3 of glutaric acid diamide had a 4-chlorophenyl or an isobutyl group.

In conclusion, I discovered *Comamonas* sp. KNK3-7, which possesses an (*R*)-selective CGD or IBD hydrolase activity, in the soil. To my knowledge, the synthesis of an (*R*)-3-substituted glutaric acid monoamide by the desymmetrization of a 3-substituted glutaric acid diamide using a microorganism and an enzyme has not been previously reported. I also succeeded in purifying *CoAM*, its gene cloning, and gene expressing. Substitution of Leu146, located in the substrate-binding pocket, with methionine resulted in substantially improved enzyme activity. Thus, *CoAM* mutants, particularly L146M, may be useful to increase the efficiency of desymmetrization of CGD. Improvements to amidase-based preparation of (*R*)-CGM, such as that demonstrated here, combined with the Hofmann rearrangement will enable more efficient chemoenzymatic synthesis of (*R*)-baclofen.

(a)



(b)

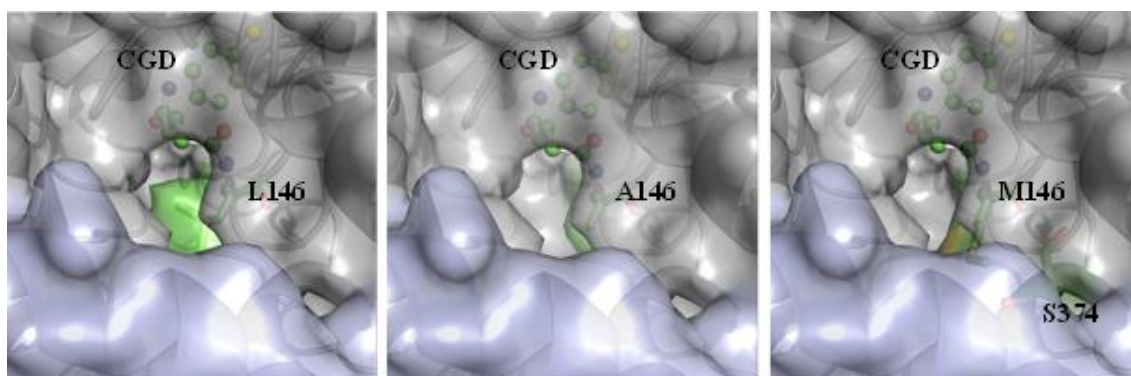


Figure 1-7. Predicted crystal structure of amidase/substrate complexes. (a) Schematic representation of the substrate-binding site in the crystal structure of a RhAmidase/benzamide complex. The two monomer components of RhAmidase are shown as cartoons, and the transparent surface is depicted in gray and purple. Phe146 is shown as sticks and its surface is highlighted in atomic colors. The bound benzamide is shown as a CPK model. (b) Schematic representation of the substrate-binding site in the modeled structures of wild-type (left), L146A mutant (center), and L146M mutant (right) *CoAM* complexed with CGD. Residue 146 and Ser-374 (shown only in the right-most panel) are highlighted in the same manner as (a). The bound CGD is shown as a CPK model.

SUMMARY

Microorganisms were screened for their ability to produce (*R*)-3-(4-chlorophenyl) glutaric acid monoamide (CGM) from 3-(4-chlorophenyl) glutaric acid diamide (CGD) through stereoselective hydrolysis. Four CGD-assimilating microorganisms were found to be potential catalysts for (*R*)-CGM production. Among these microorganisms, *Comamonas* sp. KNK3-7 produced (*R*)-CGM with the highest optical purity (98.7% *e.e.*) and was selected as the most promising strain. The *Comamonas* sp. KNK3-7 amidase (*CoAM*) gene was cloned, sequenced, and found to comprise 1512 bp. *CoAM*-transformed *Escherichia coli* were able to perform (*R*)-selective hydrolysis of CGD; however, complete conversion of 166 mM CGD in 28 h could not be obtained. I attempted to optimize the reactivity of *CoAM* by mutating single amino acids in the substrate-binding domain. Notably, the methionine-substituted L146M mutant enzyme showed increased reactivity, completing the conversion of 166 mM CGD in just 4 h. The K_m value for L146M was lower than that of *CoAM*.

CHAPTER II

**Imidase catalyzing desymmetric imide hydrolysis forming
optically active 3-substituted glutaric acid monoamides
for gamma-aminobutyric acid (GABA) analog synthesis**

As mentioned in Chapter I, several types of gamma-aminobutyric acid (GABA) analogs, the pharmacological activities of which depend on their chirality as well as chemical composition, have been synthesized for human therapeutics.

High purity, optically active 3-substituted glutaric acid monoamides can easily be converted to their corresponding GABA derivatives through Hofmann rearrangements, making them valuable synthetic intermediates [12, 13, 14]. My aim was to develop a novel chemoenzymatic process for obtaining an optically active 3-substituted glutaric acid monoamide with an enzyme capable of asymmetrically hydrolyzing 3-substituted glutarimide in a stereoselective manner.

The glutarimide transformation pathway was first reported in the bacteria *Blastobacter* sp. A17p-4 [26] and begins with the hydrolysis of glutarimide to glutaric acid monoamide by an imidase [27]. As a result, the potential of other imidases to catalyze the enantioselective hydrolysis of 3-substituted glutarimides was investigated. In this report, I described the screening of microorganisms for imidases capable of transforming the key intermediates in the synthesis of arbaclofen, 3-(4-chlorophenyl) glutarimide (CGI), or in the synthesis of pregabalin (Lyrica[®]), 3-isobutyl glutarimide (IBI), through imide desymmetrization (Fig. 2-1). I identified an imidase, BpIH, in *Burkholderia phytofirmans* DSM17436 capable of (*R*)-selectively hydrolyzing CGI to form (*R*)-3-(4-chlorophenyl) glutaric acid monoamide (CGM). In addition, the genes encoding BpIH and a homologous imidase from *Alcaligenes faecalis* NBRC13111 were isolated, expressed in *Escherichia coli*, and characterized.

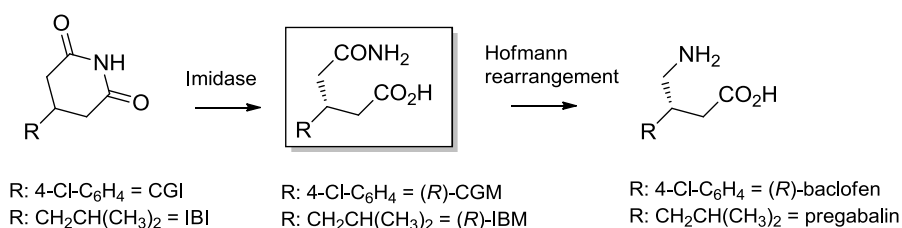


Figure 2-1. Synthesis of the intermediates of (*R*)-baclofen and pregabalin.

MATERIALS AND METHODS

Chemical reagents

CGI and IBI were prepared as described in the sections “Preparation of CGI and IBI.” (*RS*)-CGM, (*R*)-CGM, 3-(4-chlorophenyl) glutaric acid (CGA), (*RS*)-IBM, (*R*)-IBM, and 3-isobutyl glutaric acid (IBA) were prepared as described in chapter I. All other chemicals used in this study were of analytical grade and available from commercial sources.

Preparation of CGI and IBI

A mixture of urea (15.0 g; 250 mmol) and CGA (24.3 g; 100 mmol) was heated at 160 °C and stirred for 1 h. It was cooled to 90 °C, 83 mL of distilled water was added, and it was stirred for 10 min. Next, the reaction mixture was cooled to 25 °C and stirred for 1 h. The resulting solid was filtered and dried under reduced pressure. Toluene (35 mL) was added to the solid; the mixture was stirred at 90 °C for 10 min and followed by cooling to 25 °C and stirring for 1 h. An ammonia solution (10 mL, 25% (w/v)) was added to the resulting reaction slurry, and the mixture was stirred at 25 °C for 30 min. The final solid precipitate was collected by filtration and dried under reduced pressure to yield CGI (17.9 g; 79.9 mmol) as a white solid. The product was analyzed by proton NMR for structural integrity: ¹H-NMR (CDCl₃) δ (ppm): 2.72 (2H, m), 2.91 (2H, m), 3.41 (1H, m), 7.16(2H, d), 7.36 (2H, d), 7.94 (1H, br).

A mixture of urea (14.3 g; 238 mmol) and IBA (19.2 g, 95.0 mmol) was heated at 160 °C and stirred for 1 h. It was cooled to 90 °C, and distilled water (79 mL) was added. After 10 min of stirring at 90 °C, the reaction mixture was cooled to 25 °C and stirred for 1 h. The obtained solid was filtered and dried at reduced pressure. Fifty milliliters of 25% (w/v) ammonia solution was added to the solid, and the mixture was stirred at 25 °C for 1 h. The resulting solid precipitate was collected by filtration and dried under reduced pressure to yield IBI (10.5 g; 61.9 mmol) as a white solid. The product was analyzed by proton NMR for structural integrity and found to match literature values: ¹H-NMR (CDCl₃) δ (ppm): 0.91 (6H, d), 1.26 (2H, m), 1.67 (1H, m), 2.23 (3H, m), 2.70 (2H, m), 7.94 (1H, br) [28].

Microorganisms and plasmids

Bacteria were obtained from the culture collection of the Faculty of Agriculture, Kyoto University (AKU) as the type strains and from the succinimide-assimilating strains stored in my

laboratory. The *E. coli* JM109 used as the host for gene cloning and protein expression was purchased from Takara Bio (Shiga, Japan). The pQE60 vector was purchased from Qiagen (Hilden, Germany).

Culture conditions

The bacterial culturing media used for the screening consisted of 0.5% (w/v) Bacto™ Tryptone, 0.1% (w/v) D-glucose, 0.5% (w/v) yeast extract, and 0.1% (w/v) K₂HPO₄ (pH 7.0). The TGY media consisted of 0.5% (w/v) Bacto™ Tryptone, 0.1% (w/v) D-glucose, and 0.5% (w/v) yeast extract (pH 7.0). The LB media consisted of 1% (w/v) Bacto™ Tryptone, 0.5% (w/v) Bacto™ Yeast Extract, and 0.5% (w/v) NaCl (pH 7.0). When necessary, ampicillin (0.05 mg/mL) was added to the media.

Screening for (*R*)-CGM-producing strains

Each strain was inoculated into a culture tube containing 5 mL of medium and incubated for 1-4 days at 30 °C with shaking. The cells from each 5 mL culture were harvested via centrifugation and resuspended in 0.2 mL of 100 mM potassium phosphate buffer (pH 7.0). The resulting cell suspensions (0.5 mL each) were separately mixed with 2.5 mg CGI (22.4 mM) synthesized by the method described in “Preparation of CGI,” and the reaction mixtures were stirred at 30 °C. Aliquots of the reaction mixtures were withdrawn after 24 h and analyzed by HPLC (as described in “Analytical methods”) to determine the conversion rate (%) of the substrate (CGI) to the product (CGM) in the reaction solution and the optical purity by enantiomeric excess (% *e.e.*) of CGM.

Evaluation of IBI hydrolysis

Cell suspensions (0.5 mL each), prepared as described under “Screening of (*R*)-CGM-producing strains,” were separately mixed with 2.5 mg IBI (29.5 mM) and stirred at 30 °C. After 22 h, aliquots of the reaction mixtures were withdrawn and analyzed by HPLC (as described in “Analytical methods”) to determine the conversion rate (%) of the substrate (IBI) to the product (IBM) in the reaction solution and the optical purity (% *e.e.*) of IBM.

Enzyme assays

During the purification of the imidases, enzyme assays were performed with CGI as a substrate to determine active fractions after column elution and when determining specific activities for each purification step. The standard reaction mixture (0.06 mL) contained 100mM potassium phosphate buffer (pH 7.0), 4.5 mM CGI, and an appropriate amount of the enzyme. After the reaction was monitored at 28 °C for 1 h, the amount of CGM was determined using the HPLC method described in “Analytical methods.” One unit of the enzyme was defined as the amount needed to catalyze the formation of 1 μ mol of CGM in 1 min. Protein concentrations were determined by Quick Start™Bradford Dye Reagent (Bio-Rad Laboratories KK, Tokyo, Japan).

Analytical methods

¹H-NMR spectra were recorded in CDCl₃ using a JM-400 FT-NMR spectrometer (400 MHz; Jeol, Japan). Chemical shifts are expressed in parts per million (ppm), with tetramethylsilane (TMS) as the internal standard.

The degree of conversion of CGI to CGM and IBI to IBM was analyzed by reversed-phase HPLC using a Shimadzu LCVP system (Shimadzu Scientific Instruments, Kyoto, Japan) equipped with a Cosmosil 5C18-AR-II column (4.6 × 250mm; Nacalai Tesque, Kyoto, Japan). HPLC was conducted using acetonitrile/water (4:6 by vol., pH 2.5, adjusted with phosphoric acid) as the mobile phase, a flow rate of 0.5 mL/min, a column temperature of 30 °C, and ultraviolet (UV) detection at 210 nm. The retention times of CGM, CGA, and CGI were 7.1, 10.1, and 14.5 min, respectively. The retention times of IBM, IBA, and IBI were 6.7, 9.2, and 11.8 min, respectively.

The optical purity (% *e.e.*) of CGM was determined by reversed-phase HPLC using a Shimadzu LC-VP system equipped with two Sumichiral OA-7000 columns (4.6 × 250 mm; Sumika Chemical Analysis Service Ltd., Osaka, Japan). HPLC runs were conducted using acetonitrile/ water (2:8 by vol., pH 2.5, adjusted with phosphoric acid) as the mobile phase, a flow rate of 0.5 mL/min, a column temperature of 30 °C, and UV detection at 210 nm. The retention times of (*S*)-CGM, (*R*)-CGM, and CGI were 33.0, 35.1, and 41.5 min, respectively.

To determine the optical purity of IBM, the IBM in the reaction solution was derivatized using phenacyl bromide, and the obtained derivatives were analyzed. The

derivatization procedure was as follows. The K_2CO_3 (30 mg), acetonitrile (400 mg), and phenacyl bromide (10 mg) were added to the reaction mixture (100 mg). The mixture was stirred for 15 min, separated by thin-layer chromatography (hexane/acetone, 3:1 by vol., R_f value = 0.08, Merck, Darmstadt, Germany), and the derivatives were extracted by ethyl acetate. The solution was concentrated under reduced pressure to remove ethyl acetate and dissolved in water. The diluted solution was considered to contain the IBD derivatives.

The determination of the optical purity (% *e.e.*) of the IBM derivatives was performed by reverse-phase HPLC using a Shimadzu LC-VP system equipped with a Chiralpack AD-RH column (4.6 × 150 mm; Daicel, Osaka, Japan). HPLC runs were conducted using acetonitrile/water (1:1 by vol., pH 2.5, adjusted with phosphoric acid) as the mobile phase, a flow rate of 0.5 mL/min, a column temperature of 30 °C, and UV detection at 210 nm. The retention times of (*S*)-IBM and (*R*)-IBM were 12.7 and 14.6 min, respectively.

Purification of imidase BpIH from *B. phytofirmans* DSM17436

B. phytofirmans DSM17436 was subcultured in 3 mL of TGY medium at 28 °C for 22 h in a culture tube. A 3-mL subculture was used to inoculate each of 10 Sakaguchi flasks, containing 500 mL of TGY media. After a 30 h incubation at 28 °C with reciprocal shaking, *B. phytofirmans* DSM17436 cells were collected by centrifugation from 5 L of the cultured broth (from ten Sakaguchi flasks), and suspended in 100 mL of 20 mM potassium phosphate (pH 7.5).

All purification procedures were performed at 4 °C. After ultrasonic disruption of the cells, using an Insonator 201M (Kubota, Tokyo, Japan) at a power of 170 W for 30 min, 95 mL of cell-free extract was obtained by centrifugation. Ammonium sulfate was added to the cell-free extract to reach a saturation concentration of 20%, and the mixture was stirred for 0.5 h. The precipitate was discarded after centrifugation. A second ammonium sulfate cut was made of the supernatant to reach a saturation concentration of 40%. After 0.5 h of stirring, the mixture was centrifuged, the supernatant discarded, the precipitate was suspended in 85 mL of 20 mM potassium phosphate (pH 7.5) and dialyzed with 20 mM Tris-HCl (pH 7.5).

All chromatography columns used in the purification of BpIH were pre-equilibrated with 20 mM Tris-HCl (pH 7.5), and pooled elution fractions were determined by enzymatic assays. The dialyzed enzyme solution (80 mL) was applied to a 20-mL HiPrep DEAE FF 16/10 column (GE Healthcare Bio-Sciences, Tokyo, Japan), and the enzyme was eluted with a linear

gradient of 0–1 M NaCl. Forty-five milliliters of the enzyme solution of the active fractions were collected and dialyzed with 20 mM Tris-HCl (pH 7.5). Subsequently, the enzyme solution was applied to an 8-mL MonoQ 10/100 GL column (GE Healthcare Bio-Sciences), and eluted with a 0–1 M NaCl, linear gradient. Ten milliliters of the enzyme solution from the active fractions were collected and concentrated with Amicon[®] Ultra-15 (PLGC Ultracel-PL membrane, 10 kDa MWCO, EMD Millipore, Billerica, MA, USA). Next, the concentrated enzyme solution was applied to a 24-mL Superdex 200 10/300 GL (GE Healthcare Bio-Sciences) equilibrated with 20 mM Tris-HCl (pH 7.5) containing 0.2 M NaCl. The enzyme was eluted with the equilibration buffer, and 12 mL of the enzyme solution from the active fractions were collected. To prepare the enzyme for hydrophobic chromatography, ammonium sulfate was added to a final concentration of 2.0 M, and the enzyme solution was applied to a 1-mL RESOURCE PHE column (GE Healthcare Bio-Sciences), equilibrated with the standard buffer containing 2.0 M ammonium sulfate. The enzyme was eluted with a linear 2.0–0 M ammonium sulfate gradient. Seven milliliters of the enzyme solution of the active fractions were collected and concentrated by Amicon[®] Ultra-15 (PLGC Ultracel-PL membrane, 10 kDa MWCO, EMD Millipore). This time the concentrated enzyme solution was applied to a 7.5 mm (ID) × 7.5 cm TSK gel DEAE-5PW (Tosoh, Tokyo, Japan) and eluted with a 0–1.0 M NaCl linear gradient. In total, 2.0 mL of the enzyme solution of the active fractions were collected and concentrated by Amicon[®] Ultra-15 (PLGC Ultracel-PL membrane, 10 kDa MWCO, EMD Millipore). Finally, the enzyme solution was applied to a 1-mL MonoQ 5/50 GL (GE Healthcare Bio-Sciences) equilibrated with 20 mM Tris-HCl (pH 7.5). The enzyme was eluted with a 0–1.0 M NaCl linear gradient. In total, 1.0 mL of the enzyme solution from the active fractions were collected and used as pure enzyme.

N-terminal amino acid sequencing of BpIH

To isolate purified enzyme, BpIH from SDS-PAGE (12.5%) was transferred to a PVDF membrane using a AE-8750 PowerStation 1000XP (ATTO, Tokyo, Japan), AE-6677G Holize Blot (ATTO), Extra Thick Blot Paper Mini blot size (Bio-Rad Laboratories KK), and Sequi-Blot PVDF Membrane for Protein Sequencing (Bio-Rad Laboratories KK) following the manufacturers' instructions. The sequence of BpIH immobilized onto PVDF membrane was analyzed with a model PPSQ-31B protein sequencer (Shimadzu).

Nucleotide sequencing

The nucleotides of the cloned DNA fragments were sequenced by the dideoxy chain termination method using GenomeLab Dye Terminator Cycle Sequencing with Quick Start Kit (Beckman Coulter, Brea, CA) and a CEQ 2000XL DNA Analysis System. Sequence data were analyzed by Genetyx-Win software (Genetyx, Tokyo, Japan).

Expression of *bpih* gene in *E. coli*

The DNeasy Blood & Tissue Kit (Qiagen) was used to isolate total DNA from *B. phytofirmans* DSM17436. Oligonucleotide primer pools were designed based upon the N- and C-terminal amino acid sequences of the urate catabolism protein from *B. phytofirmans* (*bpih*, GenBank: ACD16728.1). The following primers were used to amplify full-length *bpih*: 5'-GAATTCATTAAGAGGAGAAATTAACCATGCCACTCGACCCGAACTA-3' (forward) and 5'-CAACAGGAGTCCAAGCTCAGCTAATTATCATGCCGCAGCCCCGCGGT-3' (reverse). The DNA fragment was amplified by PCR using a C1000 Thermal Cycler (Bio-Rad Laboratories). The 50 µL-PCR reaction mixture was comprised of 50 ng of genomic DNA of *B. phytofirmans* DSM17436 as a template, 10 pmol of each primer, 10 nmol of dNTPs, and 1.25 units of PrimeSTAR GXL DNA Polymerase (Takara-Bio, Otsu, Japan). The thermal cycle program consisted of 98 °C for 10 s, 60 °C for 15 s, and 68 °C for 1 min for a total for 30 cycles.

The *bpih* gene fragment was ligated with pQE60 vector digested with *Hind*III and *Nco*I to form pQE60BPIH using the Gibson Assembly Master Mix (New England Biolabs Japan, Tokyo, Japan). pQE60BPIH was introduced to *E. coli* JM109, and the insert fragment was confirmed to be accurate by sequencing analysis.

Expression of *afih* gene in *E. coli*

The total DNA from *A. faecalis* NBRC13111 was isolated using a DNeasy Blood & Tissue Kit (Qiagen). Oligonucleotide primers were designed based upon the nucleotides encoding the N- and C-terminal amino acid sequences of allantoinase (*afih*, GenBank: KGP00466.1), which exhibited 75% identity with BpIH. The full-length *afih* gene was amplified with the following primers: 5'-GAATTCATTAAGAGGAGAAATTAACCATGTCCTTGAGTAAGTACCC-3' (forward)

and 5'-CAACAGGAGTCCAAGCTCAGCTAATTATCAGGCCTTGGGCTGGTAGG-3' (reverse). The DNA fragment was amplified by PCR using a C1000 Thermal Cycler. The 50 μ L PCR reaction mixture was comprised of 50 ng of genomic DNA from *A. faecalis* NBRC13111 as a template, 10 pmol of each primer, 10 nmol of dNTPs, and 1.25 units of PrimeSTAR GXL DNA Polymerase (Takara-Bio). The thermal cycling program consisted of 98 °C for 10 s, 60 °C for 15 s, and 68 °C for 1min for a total for 30 cycles.

The *afih* gene fragment was ligated with pQE60 vector digested with *Hind*III and *Nco*I using a Gibson Assembly Master Mix (New England Biolabs Japan). The resulting pQE60AFIH vector was introduced to *E. coli* JM109, and the insert sequence was confirmed to be accurate by sequencing analysis.

Purification of recombinant BpIH and AfIH

E. coli JM109 harboring pQE60BPIH or pQE60AFIH were subcultured in culture tubes containing 2 mL of LB media at 28 °C for 24 h. The subcultures (2 mL) were used to inoculate Sakaguchi flasks containing 500 mL of LB. The flasks were incubated at 28 °C for 7 h, with shaking at 120 rpm. After the addition of isopropyl- β -thiogalactopyranoside (IPTG) at final concentration of 1 mM, the cultures were incubated at 28 °C for 17 h, with shaking at 120 rpm. The cells were collected by centrifugation and suspended in 20 mM potassium phosphate (pH 7.5).

The purification schemes for BpIH and AfIH were identical, all purification procedures were performed at 4°C, all chromatography columns were pre-equilibrated with 20 mM Tris-HCl (pH 7.5), and pooled elution fractions were determined by enzymatic assays. After ultrasonic disruption of the *E. coli* JM109 with over-expressed BPIH or AFIH, using an Insonator 201M at a power of 170 W for 30 min, 20 mL of cell-free extract were obtained by centrifugation and dialyzed with 20 mM Tris-HCl (pH 7.5). The dialyzed lysate was applied to an 8-mL MonoQ 10/100 GL (GE Healthcare Bio-Sciences), and the enzyme was eluted with a linear 0–1 M NaCl gradient. Active fractions were determined from activity assays, pooled, and concentrated with Amicon[®] Ultra-15 (PLGC Ultracel-PL membrane, 10 kDa MWCO, EMD Millipore). The enzyme solution was applied to a 24-mL Superdex 200 10/300 GL (GE Healthcare Bio-Sciences) column, equilibrated with buffer containing 0.2 M NaCl. The enzyme was eluted with equilibration buffer, and the active fractions were collected. The molecular

weight of the subunit was estimated by SDS-PAGE (12.5%) in reference to SDS-PAGE markers AE-1440 EzStandard (ATTO).

Bioconversion of CGI to (R)-CGM, and IBI to (R)-IBM

The CGI reaction mixtures (0.5 mL) contained 100 mM potassium phosphate buffer (pH 7.0), 22.4 mM CGI, and 100 µg/ml of BpIH or AfIH, and the reaction mixtures were stirred at 28 °C for 16 h. The IBI reaction mixtures (0.25 mL) contained 100 mM potassium phosphate buffer (pH 7.0), 29.5 mM IBI, and 1.3 mg/ml of BpIH or AfIH, and the reaction mixtures were stirred at 28 °C for 16 h. Subsequently, aliquots of the reaction mixtures were withdrawn and centrifuged. The supernatants were analyzed by HPLC to determine the conversion degree (%) of the substrate to the product and the optical purity (% *e.e.*) by the methods described in “Analytical methods.”

Analysis of recombinant BpIH and AfIH activities

The substrate specificities of BpIH and AfIH were investigated via activity assays with the substrates CGI, IBI, phthalimide, *cis*-1,2,3,6-tetrahydrophthalimide, allantoin, 2,4-thiazolidinedione, hydantoin, dihydrouracil, glutarimide, and succinimide. The standard reaction mixture (0.1 mL) contained 100 mM potassium phosphate buffer (pH 7.5), 4 mM of each substrate, and an appropriate amount of the enzyme. After the reaction was incubated at 28 °C for 30 min, the reaction was terminated with the addition of 10 µL of 15% (v/v) perchloric acid. The reaction mixtures with allantoin, hydantoin, and dihydrouracil were centrifuged, and the supernatants were analyzed to determine the amount of product by reversed-phase HPLC using a Shimadzu LC-VP system (Shimadzu) equipped with a Cosmosil 5C₁₈-AR-II column (4.6 mm × 250 mm; Nacalai Tesque, Japan). HPLC runs were conducted using 250 mM KH₂PO₄ as the mobile phase, a flow rate of 1.0 mL/min, a column temperature of 40 °C, and UV detection at 210 nm. The reaction mixtures (excluding allantoin, hydantoin, and dihydrouracil) were centrifuged, and the supernatants were analyzed by the methods described “Analytical methods” to determine the amount of product generated.

The apparent K_m and K_{cat} values for CGI, IBI, and allantoin were calculated from Lineweaver–Burk plots resulting from the aforementioned standard activity assays with recombinant BpIH and AfIH by varying the substrate concentrations.

RESULTS

Screening for (*R*)-selective CGI-hydrolyzing bacteria

I screened 64 succinimide-assimilating and 50 type strains for the ability to stereoselectively hydrolyze CGI, and found 8 strains to produce CGM in the resting cell reactions (Table 2-1). Among the strains tested, there was no (*S*)-selective hydrolyzing strains. The production of (*R*)-CGM at an optical purity of over 90% *e.e.* was observed in two strains. The highest optical purity (98.1% *e.e.*) of (*R*)-CGM was observed in *Alcaligenes faecalis* NBRC13111, which did not produce CGA. The second highest optical purity (97.5% *e.e.*) was obtained in *Burkholderia phytofirmans* DSM17436. These two strains became the focus of my investigation for imidasases capable of (*R*)-selective hydrolysis of 3-substituted gluarimides because they generated the desired (*R*)-CGM with high enantioselectivity from CGI.

Table 2-1 Microorganisms producing (*R*)-CGM from CGI through desymmetrizing hydrolysis.

Microorganism	CGM		CGA
	Conversion (%)	Stereoselectivity (% <i>e.e.</i>)	Conversion (%)
<i>Alcaligenes faecalis</i> NBRC13111	77.3	98.1 (<i>R</i>)	Not detected
<i>Achromobacter xylosoxidans</i> subsp. denitrificans NBRC12669	22.8	62.4 (<i>R</i>)	0.4
<i>Achromobacter</i> sp. A35 AKU110	73.3	82.8 (<i>R</i>)	2.5
<i>Burkholderia phytofirmans</i> DSM17436	46.2	97.5 (<i>R</i>)	0.2
<i>Comamonas</i> sp. I3-4	61.4	83.7 (<i>R</i>)	0.8
<i>Delftia acidovorans</i> NBRC14950	17.7	12.0 (<i>R</i>)	1.5
<i>Delftia</i> sp. J3-2	53.1	85.9 (<i>R</i>)	0.3
<i>Pseudomonas putida</i> s52 AKU885	11.3	80.9 (<i>R</i>)	Not detected

Bacterial asymmetric IBI hydrolysis by *A. faecalis* NBRC13111 and *B. phytofirmans* DSM17436

After a 22-h reaction with 0.5% (w/v) IBI (29.5 mM) as the substrate and the washed cells of *B. phytofirmans* DSM17436 as catalysts, (*R*)-IBM was formed with higher optical purity (94.9% *e.e.*) than that with *A. faecalis* NBRC13111 (75.5% *e.e.*) (Table 2-2). IBA production was not observed in the reaction mixture of either strain. *B. phytofirmans* DSM17436 was selected as the most promising source of imidase, based on the activity and the stereoselectivity.

Table 2-2 Microorganisms producing (*R*)-IBM from IBI through desymmetrizing hydrolysis.

Microorganism	IBM		IBA
	Conversion (%)	Stereoselectivity (% <i>e.e.</i>)	Conversion (%)
<i>Alcaligenes faecalis</i> NBRC13111	8.8	75.5 (<i>R</i>)	Not detected
<i>Burkholderia phytofirmans</i> DSM17436	18.9	94.9 (<i>R</i>)	Not detected

Purification of CGI hydrolase from *B. phytofirmans* DSM17436

The CGI hydrolase from *B. phytofirmans* DSM17436, BpIH, was purified approximately 645-fold in seven successive steps from the cell lysate. Representative results of the purification are shown in Table 2-3. The final preparation exhibited a specific activity of 948 mU/mg and showed a single band on an SDS-PAGE gel (Fig. 2-2). The subunit molecular weight of the purified enzyme was determined to be approximately 36,000 by SDS-PAGE analysis (Fig. 2-2). Gel filtration column chromatography showed that molecular weight of the native BpIH was 117,000.

Table 2-3 Purification of CGI hydrolase (BpIH).

Step	Total volume (mL)	Total protein (mg)	Total activity (mU) ^a	Yield (%)	Specific activity (mU/mg)	Purification (fold)
Cell-free extract	95	2150	3180	100	1	1
Ammonium sulfate precipitation	80	1100	2900	91	3	2
Hiprep DEAE FF 16/10	45	343	2090	66	6	4
MonoQ 10/100 GL	10	62	755	24	12	8
Superdex 200 10/300 GL	12	35	719	23	21	14
Resource PHE	7	9	564	18	65	44
TSKgel DEAE-5PW	2	0.4	233	7	597	406
MonoQ 5/50 GL	1	0.1	57	2	948	645

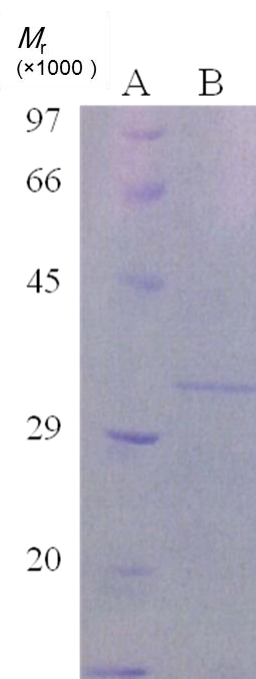


Figure 2-2. Representative results of SDS-PAGE analysis (12.5%) of the purified BpIH from *Burkholderia phytofirmans* DSM17436. Molecular weight markers were used to estimate the molecular weight of 36,000 for BpIH. (A) Protein molecular weight markers. Corresponding weights are indicated to the left of each protein band. (B) Purified BpIH.

Sequence analysis of the BpIH and allantoinase from *A. faecalis* NBRC13111

The N-terminal amino acid sequence of BpIH was determined to be: PLDPNYPRDL. The sequence exhibited 100% identity with the urate catabolism protein from *B. phytofirmans* DSM17436 (GenBank: ACD16728.1). The ORF of the *bpih* gene consists of 951 bp, including the initiation (ATG) and stop (TGA) codons, encoding a protein of 316 amino acid residues. The predicted molecular weight of 36,471 was nearly identical to the molecular weight of 36,000 estimated for the purified BpIH. The amino acid sequence of BpIH was compared with other protein sequences using the BLAST search tool (<http://www.genome.jp/tools/blast/>). Database analysis revealed that BpIH exhibited high amino acid sequence identity (75%) with allantoinase from *A. faecalis* NBRC13111 (AfiH, GenBank: KGP00466.1). The ORF of the *afih* gene consisted of 933 bp including the initiation (ATG) and stop (TGA) codons, encoding a protein consisting of 310 amino acid residues.

Bioconversion of CGI to (*R*)-CGM and IBI to (*R*)-IBM with purified recombinant BpIH and AfiH

E. coli JM109 transformed with pQE60BPIH or pQE60AFIH, expressing recombinant BpIH and AfiH, were cultured, and the overexpressed recombinant proteins were purified. The stereoselectivity of each recombinant protein for CGI and IBI was examined and compared. The enantioselectivity of these enzymes in CGI and IBI hydrolysis are presented in Table 2-4. BpIH catalyzed the hydrolysis of both CGI and IBI with high (*R*)-selectivity (98.7% *e.e.* and 95.3% *e.e.* for CGM and IBM, respectively). AfiH catalyzed the hydrolysis of CGI with high *R*-selectivity with 97.1% *e.e.* for CGM. In contrast, AfiH hydrolyzed IBI with a lower level of enantioselectivity (89.4% *e.e.* for IBM).

Table 2-4 Bioconversion of CGI to (*R*)-CGM, and IBI to (*R*)-IBM by purified recombinant BpIH and AfiH.

Recombinant enzyme	CGM		IBM	
	Conversion (%)	Stereoselectivity (% <i>e.e.</i>)	Conversion (%)	Stereoselectivity (% <i>e.e.</i>)
BpIH	65.8	98.7 (<i>R</i>)	64.6	95.3 (<i>R</i>)
AfiH	66.2	97.1 (<i>R</i>)	50.8	89.4 (<i>R</i>)

Substrate specificity of BpIH and AfiH

To investigate the substrate specificities of the purified recombinant BpIH and AfiH, the hydrolysis of ten kinds of substrates were assayed (Table 2-5). Among the compounds tested, CGI, IBI, phthalimide, *cis*-1,2,3,6-tetrahydrophthalimide, allantoin, and 2,4-thiazolidinedione were hydrolyzed by both BpIH and AfiH. Hydantoin, dihydrouracil, glutarimide, and succinimide were not hydrolyzed by either enzyme. The K_m and K_{cat} values of BpIH and AfiH for CGI, IBI, and allantoin are shown in Table 2-6.

Table 2-5 Substrate specificities of recombinant BpIH and AfIH.

Substrate	Relative activity (%)	
	BpIH	AfIH
3-(4-Chlorophenyl) glutarimide (CGI)	100	100
3-Isobutyl glutarimide (IBI)	3	3
Phthalimide	157	174
<i>cis</i> -1,2,3,6-Tetrahydrophthalimide	22	15
Allantoin	50	58
2,4-Thiazolidinedione	22	8
Hydantoin	Not detected	Not detected
Dihydrouracil	Not detected	Not detected
Glutarimide	Not detected	Not detected
Succinimide	Not detected	Not detected

Table 2-6 Kinetic properties of recombinant BpIH and AfIH in CGI, IBI, and allantoin hydrolysis.

Substrate	BpIH		AfIH	
	K_m (mM)	K_{cat} (1/sec)	K_m (mM)	K_{cat} (1/sec)
3-(4-Chlorophenyl) glutarimide (CGI)	2.2	6.3	2.9	6.2
3-Isobutyl glutarimide (IBI)	1.3	0.005	1.4	0.005
Allantoin	29	760	36	100

Effects of pH and temperature on recombinant BpIH and AfIH

The optimal pH for the hydrolysis of CGI by BpIH and AfIH was investigated, revealing maximal activity for both at pH 9.0 (Figs. 2-3 and 2-4, respectively). Each enzyme reaction was examined at various temperatures (10–70 °C) at pH 7.5, and both enzymes were maximally active at 50 °C (Figs. 2-5 and 2-6). The thermal stability of the enzymes was examined at a range of temperatures (4–70 °C) for 30 min at pH 7.5. The results demonstrated that both enzymes were stable below 40 °C as described in Figs. 2-5 and 2-6. The pH stability for both enzymes was determined to be within the range of pH 6.0–10.0 by incubating them at 4 °C for 30 min in various buffers and assaying the remaining activity (Fig. 2-7).

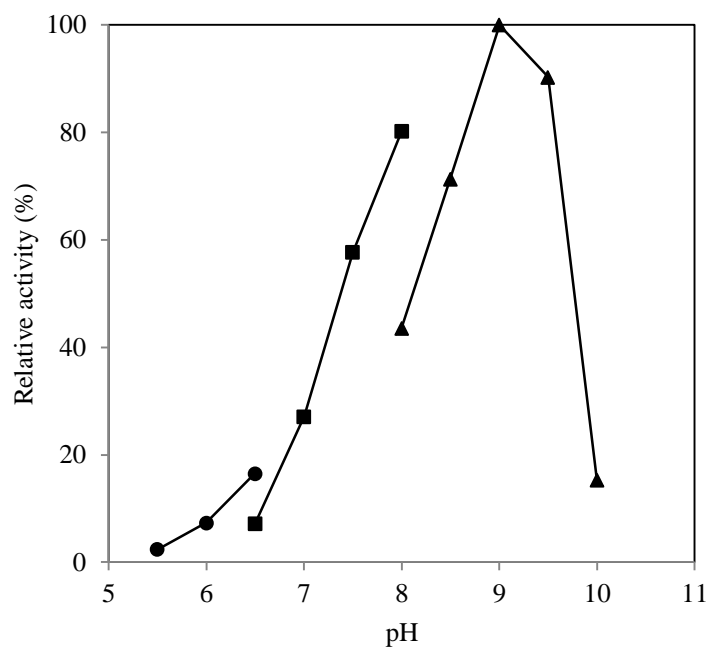


Figure 2-3. Effects of pH on the activity of BpIH. The effects of the pH of the reaction buffer on recombinant BpIH enzymatic activity with the substrate CGI are shown. The percent relative activities were calculated from the maximal enzyme activity (pH 9.0). Assays were monitored under the standard reaction conditions as described in “Analysis of recombinant BpIH and AfIH activity” with the following exceptions. The pH of the reaction mixture was adjusted with the use of the following buffers: *circles*, 100 mM MES/NaOH buffer for pH 5.5–6.5, *squares*, 100 mM potassium phosphate buffer for pH 6.5–8.0, *triangles*, 100 mM boric acid/KCl/NaOH buffer for pH 8.0–10.0.

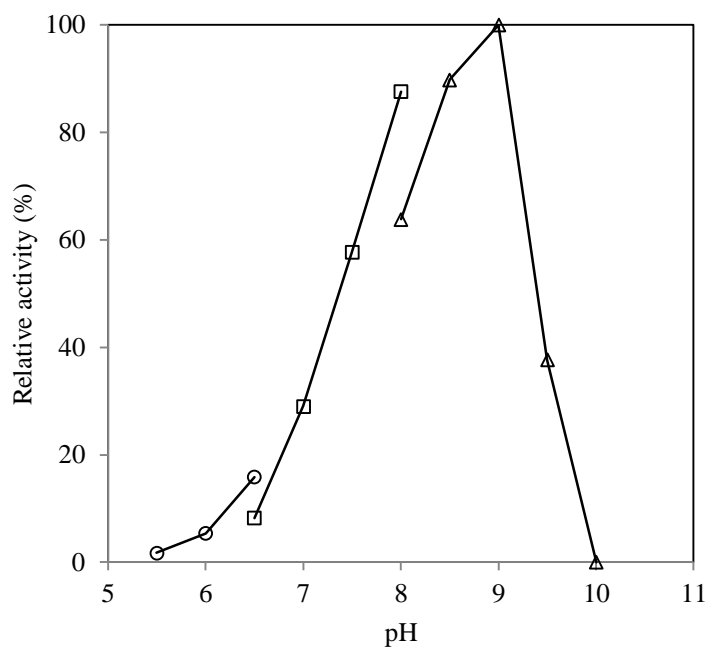


Figure 2-4. Effects of pH on the activity of AfIH. The effects of the pH of the reaction buffer on the AfIH enzymatic activity with the substrate CGI are shown. The percent relative activities were calculated from the maximal enzyme activity (pH 9.0). Assays were monitored under the standard reaction conditions as described in “Analysis of recombinant BpIH and AfIH activity” with the following exceptions. The pH of the reaction mixture was adjusted with the use of the following buffers: *circles*, 100 mM MES/NaOH buffer for pH 5.5–6.5, *squares*, 100 mM potassium phosphate buffer for pH 6.5–8.0, *triangles*, 100 mM boric acid/KCl/NaOH buffer for pH 8.0–10.0.

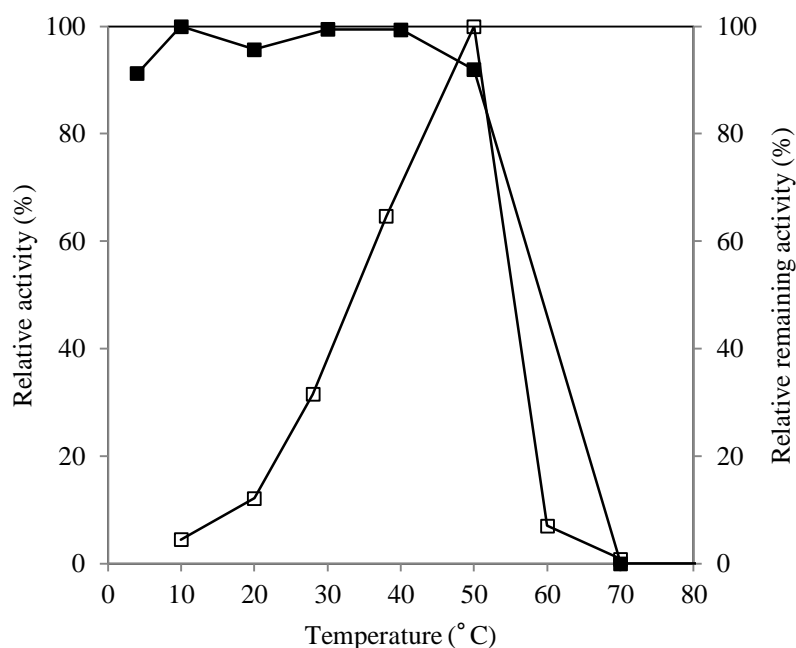


Figure 2-5. Effects of temperature on the activity and stability of BpIH. The activity of recombinant BpIH was assayed with CGI as a substrate under the standard reaction conditions as described in “Analysis of recombinant BpIH and AfIH activity” with the following exceptions. The effects of temperature on enzymatic activity were determined by varying the reaction temperatures from 10-70 °C. The heat stability studies were performed by incubating the purified enzyme solutions for 30 min at the desired temperature followed by assaying for activity. The percent relative activity was determined from the maximal enzyme activity (50 °C). The percentage of relative remaining activity was obtained as a ratio to that without heating. *Open squares*, effect of temperature on the activity; and *closed squares*, heat stability.

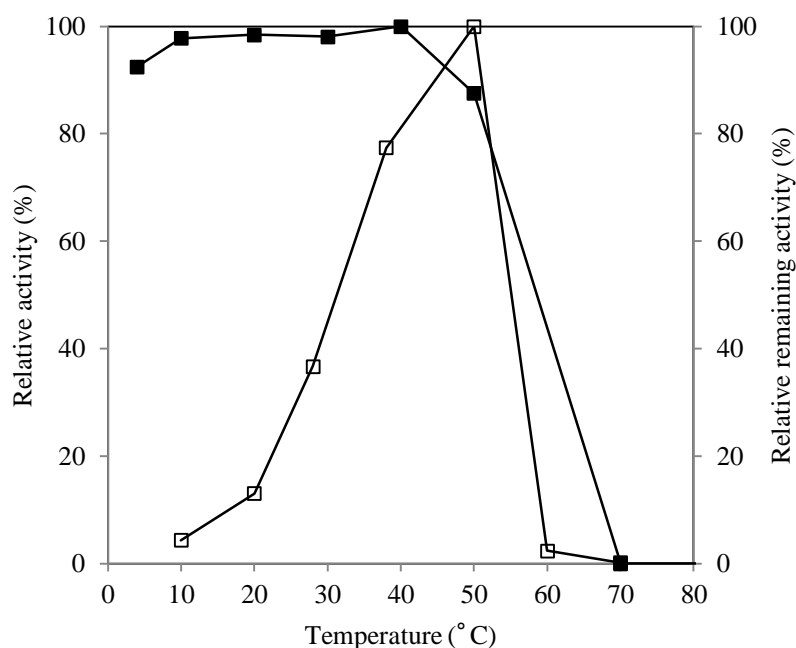


Figure 2-6. Effect of temperature on the activity and stability of the AfIH. The activity of AfIH was assayed with CGI as a substrate under the standard reaction conditions as described in “Analysis of recombinant BpIH and AfIH activity” with the following exceptions. The effects of temperature on enzymatic activity were determined by varying the reaction temperatures from 10-70 °C. The heat stability studies were performed by incubating the purified enzyme solutions for 30 min at the desired temperature followed by assaying for activity. The percent relative activity was determined from the maximal enzyme activity (50 °C). The percentage of relative remaining activity was obtained as a ratio to that without heating. *Open squares*, effect of temperature on the activity; and *closed squares*, heat stability.

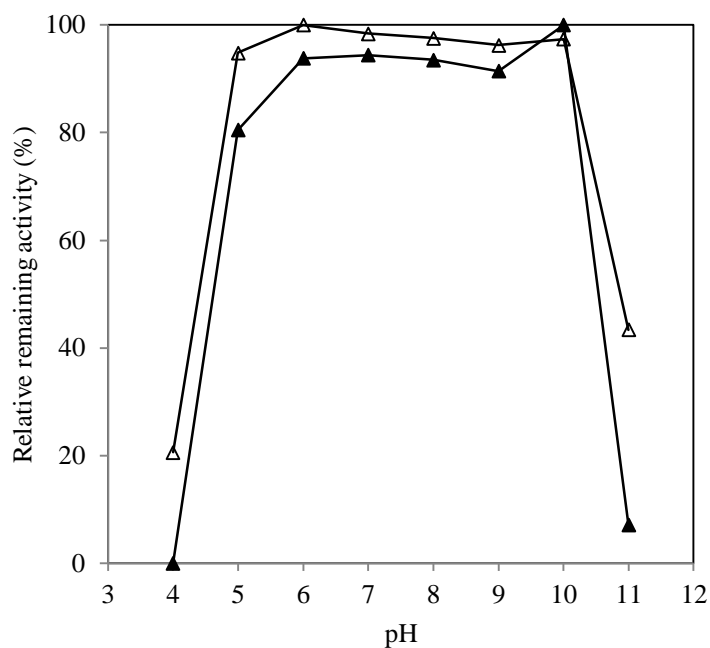


Figure 2-7. Effects of pH at 4 °C on the stability of BpIH and AfiH. The pH stability studies were performed with the incubation of purified enzyme solutions with the following reaction buffers: 80 mM acetate/sodium acetate buffer for pH 4.0–5.0, 80 mM MES/NaOH buffer for pH 6.0, 80 mM potassium phosphate buffer for pH 7.0–8.0, 80 mM boric acid/KCl/NaOH buffer for pH 9.0–10.0, and 80 mM CAPS/NaOH buffer for pH 11.0 for 30 min at 4 °C, followed by standard activity assays with CGI as a substrate as described in “Analysis of recombinant BpIH and AfiH activity.” The percentage of relative remaining activity was obtained as a ratio to that with pH 10 (BpIH) or pH 6 (AfiH). *Closed triangles*, BpIH pH stability; and *open triangles*, AfiH pH stability.

Effects of metal ions on the enzymatic activity

The effects of various metal ions (1 mM) on BpIH or AfIH activity were examined. Ag^+ , Hg^{2+} , Cu^{2+} , Zn^{2+} , and Cd^{2+} inhibited both enzymes. The metal ion chelator, ethylenediaminetetraacetic acid (EDTA), showed no significant influence on the activity (Table 2-7).

Table 2-7 Effects of metal ions on recombinant BpIH and AfIH activities.

Additive ^b	Relative activity (%) ^a	
	BpIH	AfIH
None	100	100
EDTA	100	106
NaCl	104	111
AlCl_3	102	110
MgCl_2	102	113
KCl	105	112
CaCl_2	97	110
FeSO_4	93	97
MnCl_2	103	101
CoCl_2	105	106
NiCl_2	106	102
CuCl_2	9	1
ZnCl_2	100	77
Na_2MoO_4	108	106
CdCl_2	88	41
SnCl_2	103	97
HgCl_2	7	6
$\text{Pb}(\text{NO}_3)_2$	99	101
CrCl_3	108	105
AgNO_3	57	49

^aActivity is represented as a percentage of the enzyme activity without the additive reagent.

^bThe effects of various metals on the enzyme activities with CGI as a substrate were evaluated with the standard assay conditions as described in “Analysis of recombinant BpIH and AfIH activity” coupled with the addition of 1 mM of either a chelating reagent (EDTA) or metal solutions.

DISCUSSION

In this paper, I describe the discovery of bacteria that synthesize an (*R*)-3-substituted glutaric acid monoamide through the desymmetrizing hydrolysis of a 3-substituted glutarimide. To my knowledge, with the exception of the imidase catalyzed regiospecific hydrolysis of imide derivatives reported for *Arthrobacter ureafaciens* O-86 [29], the synthesis of chiral compounds by desymmetrizing hydrolysis of imide derivatives by microorganisms has not been previously reported. Other studies have reported that the expression of imidase from *Blastobacter* sp. A17p-4 is induced by some cyclic imides, such as succinimide and glutarimide [26]. However, the imide-hydrolyzing activities of the microorganisms described in my study were constitutively expressed, without the addition of imide compounds to the culture medium. This suggests that these enzymes are part of a different metabolic pathway from that of the previously reported imidase pathway [30].

BpIH and AfIH from *B. phytofirmans* DSM17436 and *A. faecalis* NBRC13111, respectively, were successfully identified, cloned, and recombinantly expressed in *E. coli*. Their identities were confirmed by querying the genome sequence database entries of their source organisms, where they were annotated as urate catabolism protein (BpIH) and allantoinase (AfIH). The amino acid sequences of BpIH and AfIH were 75% identical. BpIH and AfIH did not exhibit great differences in substrate specificity. Together with the allantoinase activity, this study demonstrates that these enzymes catalyze the desymmetrizing hydrolysis of 3-substituted glutarimides. The discovery that BpIH and AfIH could use CGI and IBI as substrates, despite lacking specificity for glutarimide, is interesting. Enzymatic activity of both enzymes with IBI was approximately 3% that of CGI, suggesting that the composition of the 3-substitution may influence activity. Importantly, BpIH enabled the highly (*R*)-selective hydrolysis of both CGI and IBI, whereas AfIH displayed low (*R*)-selectivity for IBI. Future studies should focus on the use of protein engineering techniques to obtain BpIH mutants displaying increased activity toward IBI, as well as AfIH mutants expressing high (*R*)-selectivity for IBI.

BpIH and AfIH did not exhibit great differences in their kinetic values K_m and K_{cat} for CGI, IBI, and allantoin. The CGI hydrolyzing activities of BpIH and AfIH were shown to be relatively insensitive to zinc, cobalt, and nickel ions, whereas these ions effectively activated the activity of the metal dependent *E. coli* allantoinase [31]. In addition, BpIH and AfIH activity remained unaffected by EDTA. Therefore, my results suggested that BpIH and AfIH are metal

independent enzymes.

BpIH and AfIH displayed 61% and 63% identity, respectively, with the amino acid sequence of the previously reported PuuE, allantoinase (GenBank: ACA50280.1) from *Pseudomonas fluorescens*, which catalyzes the hydrolysis of the amide bond of allantoin to form allantoic acid [32] (Fig. 2-8). It has been reported that the PuuE from *P. fluorescens* exhibits metal independent allantoinase activity in the purine catabolic pathway and stereospecificity for the (*S*)-enantiomer of allantoin. Therefore, the PuuE, like BpIH and AfIH, is expected to catalyze the desymmetrizing hydrolysis of 3-substituted glutarimides. Proteins annotated as PuuE have been reported to exist in other microorganisms [32]. The results of my study suggest that there is a possibility that this class of enzyme can be used to produce chemicals.

This study indicates that preparation of various optically active 3-substituted glutaric acid monoamides is possible by using imide-hydrolyzing enzymes. By utilizing the Hofmann rearrangement, an optically active 3-substituted glutaric acid monoamide can be converted into the corresponding optically active 3-substituted GABA. This approach could be useful for the stereoselective synthesis of related 3-substituted GABA analogs or their derivatives. Therefore, imidase is expected to be the enzyme used for the chemoenzymatic synthesis of various types of chiral GABAs. Further detailed studies are needed for practical application of BpIH to the chiral production of 3-substituted glutaric acid monoamides on an industrial scale.

```

BpIH  1  MPLDPNYPRDLIGYGRHPVQANWPGRARVAVQFVLNVEEGGENCVLHGDPGSECFLSEIVGAASFP-ARHMSMESIYEYG  79
AfIH  1  MSLS-MYPRDLVGYGKNVPHAQWPDRAHIAVQFVLNVEEGGENCVLHGDPGSECFLSEIIGAAAYP-DRHLSMESIYEYG  78
PuuE  1  MSVD--YPRDLIGYGSNPPHPWPGHARTALS FVLNVEEGGERNILHGDKESBAFLSEMVSAQPLQGERNMSMESIYEYG  78

BpIH  80  SRAGVWRILREFEKRKLELTVFEGVGMVVRHPELARAFVELGHEIACHGYRWIHYQDMAPEKEBEHMRGLGMEAIERTVTE  159
AfIH  79  SRAGVWRILNFEKRGLEPMTVEVGMALERHPELAQEFVRIHGHEIACHGYRWIHYQNVSEEVEREHMRQCCKVLTDLLEGH  158
PuuE  79  SRAGVWRILKLFKAFDIPLTTFAVVMAACRHPDVIRAMVAAGHEICSHGYRWIDYQYMDEACERHMLEAIRILTELTGE  158

BpIH  160  RFLGWYTGGRDSPNTRRLVAEYGGFLYDSDNYGDDLPEWMDVDVTGGAKVPCQLIVPYTLDDNMDRFASFGGFNTADHFFLY  239
AfIH  159  HPEGWYTGGRDSPNTRRLVAEEGCFLYSSDNYGDDLPEWTEVQLSDNTVPCQLIVPYTLDSNDMRFAPAFQGFNTGDEFFSY  238
PuuE  159  RFLGWYTGRTGPNTRRLVMEEGCFLYDSDNYGDDLPEWEPNPTG---KPELVIPYTLDDNMDRFTQVQGFNKGDEFFSY  235

BpIH  240  LRDAFDVLYEGLAEAPKMLSIGMHCRLLGRPGRFRALQRFLDHIEQHORVWVTRRVDIARHWREHHPYQNNRGAAGA  316
AfIH  239  LRDAFDVLYEGLAEAPKMLSIGLHCRLLGRPGRFRALQRFLDYVQSHERVVWQRRVDIARHWAHHPYQPKA  310
PuuE  236  LRDAFDVLYEGLAEAPKMLSIGLHCRLLGRPARLAALQRFIEYAKSHEQVWFTRRVDIARHWATHHPYTGAAK  308

```

Figure 2-8. Comparison of the amino acid sequences of the BpIH, AfIH and PuuE. Identical amino acids among the sequences are marked in black. BpIH, an urate catabolism protein of *Burkholderia phytofirmans* DSM17436 (GenBank: ACD16728.1), AfIH, an allantoinase of *Alcaligenes faecalis* NBRC13111 (GenBank: KGP00466.1), PuuE, an allantoinase of *Pseudomonas fluorescens* (GenBank: ACA50280.1).

SUMMARY

The recent use of optically active 3-substituted gamma-aminobutyric acid (GABA) analogs in human therapeutics has identified a need for an efficient, stereoselective method of their synthesis. Here, bacterial strains were screened for enzymes capable of stereospecific hydrolysis of 3-substituted glutarimides to generate (*R*)-3-substituted glutaric acid monoamides. The bacteria *Alcaligenes faecalis* NBRC13111 and *Burkholderia phytofirmans* DSM17436 were discovered to hydrolyze 3-(4-chlorophenyl) glutarimide (CGI) to (*R*)-3-(4-chlorophenyl) glutaric acid monoamide (CGM) with 98.1% *e.e.* and 97.5% *e.e.*, respectively. *B. phytofirmans* DSM17436 could also hydrolyze 3-isobutyl glutarimide (IBI) to produce (*R*)-3-isobutyl glutaric acid monoamide (IBM) with 94.9% *e.e.* BpIH, an imidase, was purified from *B. phytofirmans* DSM17436, and found to generate (*R*)-CGM from CGI with specific activity of 0.95 U/mg. The amino acid sequence of BpIH had a 75% sequence identity to that of allantoinase from *A. faecalis* NBRC13111 (AfIH). The purified recombinant BpIH and AfIH catalyzed (*R*)-selective hydrolysis of CGI and IBI. In addition, a preliminary investigation of the enzymatic properties of BpIH and AfIH revealed that both enzymes were stable in the range of pH 6–10, with an optimal pH of 9.0, stable at temperatures below 40 °C, and were not metalloproteins. These results indicate that the use of this class of hydrolase to generate optically active 3-substituted glutaric acid monoamide could simplify the production of specific chiral GABA analogs for drug therapeutics.

CHAPTER III

Characterization and application of an enantioselective amidase from *Cupriavidus* sp.

(*R*)-3-Aminopiperidine is a common intermediate in the synthesis of dipeptidyl peptidase-4 (DPP-4) inhibitors, which comprise a class of oral antidiabetic drugs [6, 7]. Therefore, the establishment of the efficient synthesis of (*R*)-3-aminopiperidine on an industrial scale is required. (*R*)-3-piperidinecarboxamide with high optical purity is a valuable synthetic intermediate because it is expected to be converted to (*R*)-3-aminopiperidine using the Hofmann rearrangement. Therefore, I sought to develop a novel biocatalytic process for obtaining (*R*)-3-piperidinecarboxamide in high enantiomeric excess using an (*S*)-selective amidase. An (*R*)-selective amidase from *Pseudomonas* sp. that could act on (*RS*)-3-piperidinecarboxamide has been reported, but the enantiomeric excess of the corresponding (*S*)-3-piperidinecarboxamide or (*R*)-3-piperidinecarboxylic acid was not described [33]. In this study, I screened for microorganisms that can selectively hydrolyze the (*S*)-enantiomer in (*RS*)-*N*-benzyl-3-piperidinecarboxamide (BNPD) (Fig. 3-1) and identified the amidase activity in *Cupriavidus* sp. KNK-J915 (FERM BP-10739). The amidase purified from cells of the strain (*S*)-selectively hydrolyzed (*RS*)-BNPD to form (*R*)-BNPD, and the enzyme was referred to as *CsAM*. *CsAM* was characterized and found to be a novel amidase with unique substrate specificity. The gene encoding *CsAM* was isolated, sequenced, and expressed in *Escherichia coli*.

Furthermore, I also report the successful synthesis of (*R*)-isovaline by the Hofmann rearrangement using highly enantiomerically pure (*S*)-2-ethyl-2-methyl-malonamic acid, prepared by *CsAM* (Fig. 3-2). (*R*)-isovaline, an optically active form of isovaline, has been reported to activate the metabotropic GABA_B receptor and act as an analgesic amino acid [34], and it has potential applications in drug development.

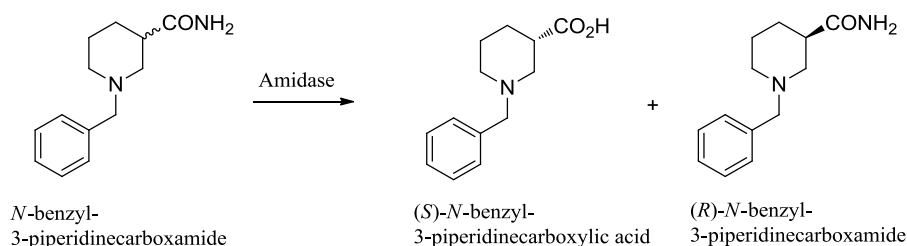


Figure 3-1. Stereoselective hydrolysis of N -benzyl-3-piperidinecarboxamide.

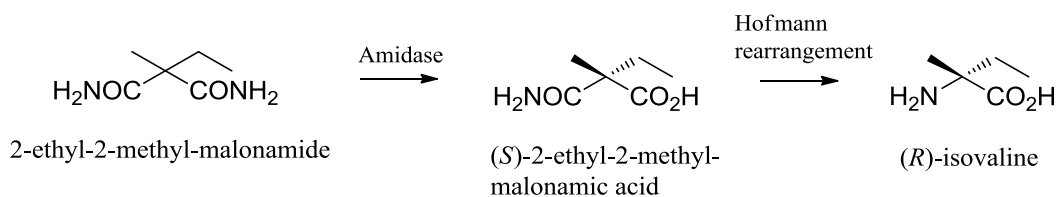


Figure 3-2. Chemoenzymatic production of (R) -isovaline.

MATERIALS AND METHODS

Chemical reagents

BNPD, (R) -BNPD, (R) - N -benzyloxycarbonyl-3-piperidinecarboxamide, (RS) - N -benzyl-3-piperidinecarboxylic acid (BNPA), (RS) -piperidine-2-carboxamide, (RS) -indoline-2-carboxylic acidamide, DL-phenylalanine amide, DL- β -phenylalanine amide, (RS) -mandelic acid amide, and (RS) -2-phenylpropionic acidamide were prepared according to existing methods. Piperidine-4-carboxamide was purchased from Sigma–Aldrich Co. LLC. (RS) -3-Piperidinecarboxamide (NPD), and (RS) -3-piperidine-carboxylic acid (NPA) were purchased from Tokyo Chemical Industry Co., Ltd. (Tokyo, Japan). All other chemicals used in this study were of analytical grade and were commercially available.

Microorganisms, culture conditions, and plasmids

Microorganisms were obtained from my laboratory collection. *Cupriavidus* sp. KNK-J915 (FERM BP-10739) was selected as a microorganism capable of hydrolyzing (RS) -BNPD with S -selectivity and used as a source of enzyme and chromosomal DNA. The medium used for the screening consisted of 1% (w/v) glycerol, 0.5% (w/v) peptone, 0.3% (w/v) yeast extract, 0.3% (w/v) malt extract, and 0.1% (w/v) isovaleronitrile (pH 7.0). The CM

medium consisted of 1% (w/v) meatextract, 1% (w/v) peptone, 0.5% (w/v) yeast extract, and 0.5% (w/v) NaCl (pH 7.0). The medium P consisted of 2% (w/v) glycerol, 1% (w/v) meat extract, 1% (w/v) peptone, and 0.5% (w/v) yeast extract (pH 7.0). *E. coli* HB101 was used as the host cell for gene cloning and expression. Transformed *E. coli* was cultured at 30°C in 2-YT medium containing 1.6% (w/v) Bacto™Tryptone, 1% (w/v) Bacto™Yeast Extract, and 0.5% (w/v) NaCl (pH 7.0). When necessary, ampicillin (0.1 mg/mL) was added to the medium. Plasmid pUCNT was prepared from pUC19 and pTrc99A as previously described [16].

Screening method for (*S*)-selective BNPD-hydrolyzing microorganisms

In the screening experiments, each strain was inoculated into 8 mL of medium in a test tube (24 mm i.d. × 200 mm), followed by incubation at 30°C with reciprocal shaking for 3 days. Microorganisms were harvested by centrifugation. The cells from 8 mL of culture broth were suspended in 1 mL of 100 mM potassium phosphate (pH 7.0). The resulting cell suspensions (0.1 mL each) were separately mixed with 0.1 mL of (*RS*)-BNPD solution [9.16 mM, solved in 100 mM potassium phosphate (pH 7.0)], and the reaction mixtures were stirred at 30°C for 24 h. After the reaction, aliquots of the reaction mixtures were withdrawn and analyzed by HPLC to determine the conversion degree (%) of the substrate to the product in the reaction solution and the optical purity (% *e.e.*). The value of enantioselectivity (*E*-value) was calculated from the conversion degree (*c*) and the enantiomeric excess of the substrate (*ee_s*) was calculated according to a previously described method [35] (Eq. (1)).

$$E = \ln[(1 - c)(1 - ee_s)] / \ln[(1 - c)(1 + ee_s)] \quad (1)$$

Enzyme assay

During the purification and characterization of amidase from *Cupriavidus* sp. KNK-J915, an enzyme assay was performed with (*RS*)-BNPD as a substrate. The standard reaction mixture (0.2 mL) contained 100 mM potassium phosphate buffer (pH 7.0), 45.8 mM BNPD, and an appropriate amount of the enzyme. After the reaction was performed at 30°C for 0.5–1 h, the amount of BNPA was determined using HPLC. One unit of the enzyme was defined as the amount catalyzing the formation of 1 mol of BNPA per minute under the aforementioned condition. Protein content was determined by the Bradford method with BSA as a standard using a kit from Bio-Rad Laboratories Ltd. (Tokyo, Japan). In the

characterization of recombinant *CsAM* and *CnAM* from *E. coli* transformant experiments, each strain was inoculated into 5 mL of 2-YT medium in a test tube (24 mm i.d. × 200 mm), followed by incubation at 30°C with reciprocal shaking for 24 h. Microorganisms were harvested by centrifugation. The cells from 5 mL of culture broth were suspended in 2.5 mL of 100 mM potassium phosphate (pH 7.0). The resulting cell suspensions (0.1 mL each) were separately mixed with 0.1 mL of (*RS*)-BNPD solution [91.6 mM, solved in 100 mM potassium phosphate (pH 7.0)] or 0.1 mL of (*RS*)-NPD solution [156 mM, solved in 100 mM potassium phosphate (pH 7.0)], and the reaction mixtures were stirred at 30°C for 2 h. After the reaction, aliquots of the reaction mixtures were withdrawn and analyzed by HPLC to determine the conversion degree (%) of the substrate to the product in the reaction solution and optical purity (% *e.e.*). Enzyme activity toward other amides [each concentration was 1%, solved in 100 mM potassium phosphate (pH 7.0)] was determined by measuring the formation of ammonia using AmmoniaTest WAKO (Wako Pure Chemicals, Osaka, Japan). One unit of the enzyme was defined as the amount catalyzing the formation of 1 mol of ammonia per minute.

Analytical methods

The degree of conversion of BNPD to BNPA was analyzed by reversed-phase HPLC using a Shimadzu LC-VP system (Shimadzu, Kyoto, Japan) equipped with a YMC-A303 column (4.6 mm × 250 mm; YMC, Kyoto, Japan). HPLC was conducted using acetonitrile:water (1:9 by vol., pH 2.5, adjusted with phosphoric acid) as the mobile phase, a flow rate of 1.0 mL/min, a column temperature of 30°C, and ultraviolet (UV) detection at 210 nm. The optical purity of BNPD was determined by reversed-phase HPLC using a Shimadzu LC-VP system equipped with a CHIRALPACK AD-RH column (4.6 mm × 150 mm; Daicel, Osaka, Japan). HPLC was conducted using acetonitrile: 20 mM potassium phosphate buffer (pH 8.0; 3:7 by vol.) as the mobile phase, a flow rate of 0.5 mL/min, a column temperature of 30°C, and UV detection at 210 nm.

NPD and NPA in the reaction solution were derivatized using carbobenzoxy chloride and the obtained derivatives were analyzed. The derivatization procedure using carbobenzoxy chloride was as follows. The saturated aqueous NaHCO₃ (200 mg) was added to the reaction mixture (100 mg). The mixture was concentrated under reduced pressure to remove NH₃. Then, THF (200 mg) and carbobenzoxy chloride (25 mg) were added to the concentrated solution.

The mixture was stirred for 10 min, and then diluted with water. The diluted solution was used as NPD and NPA derivatives. The conversion degree analysis of NPD and NPA derivatives was performed by reversed-phase HPLC with a Shimadzu LC-VP system equipped with a YMC-A303 column (4.6 mm × 250 mm). HPLC was conducted using acetonitrile:water (3:7 by vol., pH 2.5, adjusted with phosphoric acid) as the mobile phase, a flow rate of 1.0 mL/min, a column temperature of 35°C, and UV detection at 210 nm. The determination of the optical purity of NPD derivatives was performed by reversed-phase HPLC using a Shimadzu LC-VP system equipped with a CHIRALPACK AD-RH column (4.6 mm × 150 mm). HPLC was conducted using acetonitrile:water (3:7 by vol., pH 2.5, adjusted with phosphoric acid) as the mobile phase, a flow rate of 0.5 mL/min, a column temperature of 30°C, and UV detection at 210 nm.

The degree of conversion of 2-ethyl-2-methyl-malonamide to 2-ethyl-2-methyl-malonamic acid and the enantiomeric excess of 2-ethyl-2-methyl-malonamic acid were analyzed by reversed-phase HPLC using a Shimadzu LC-VP system (Shimadzu, Kyoto, Japan) equipped with two SUMICHIRAL OA-7000 columns (4.6 mm × 250 mm; Sumika Chemical Analysis Service Ltd, Osaka, Japan). HPLC was conducted using acetonitrile/water (2:8 by vol, pH 2.5, adjusted with phosphoric acid) as the mobile phase, a flow rate of 1.0 mL/min, a column temperature of 30°C, and ultraviolet (UV) detection at 210 nm. The retention times of 2-ethyl-2-methyl-malonamide (EMM), (*S*)-2-ethyl-2-methyl-malonamic acid (EMA), (*R*)-EMA, and ethylmethylmalonic acid were 9.7, 17.2, 18.9, and 80.7 min, respectively. The optical purity of (*R*)-isovaline was analyzed by reversed-phase HPLC, as described previously [36], using a Shimadzu LC-VP system (Shimadzu, Kyoto, Japan) equipped with a Chirobiotic T™ column (4.6 mm × 250 mm; Advanced Separation Technologies, Inc., New Jersey, USA). HPLC was conducted using methanol/water (9:1 by vol) as the mobile phase, a flow rate of 0.8 mL/min, a column temperature of 25°C, and ultraviolet (UV) detection at 204 nm. The retention times of (*R*)-isovaline and (*S*)-isovaline were 4.0 and 8.3 min, respectively.

Purification of the BNPD-hydrolyzing enzyme CsAM from *Cupriavidus* sp. KNK-J915

Cupriavidus sp. KNK-J915 was subcultured at 30°C for 24 h in a test tube containing 8 mL of CM medium. The subculture (1 mL) was then inoculated into a 500-mL

Sakaguchi flask containing 120 mL of medium P. After a 3-day incubation at 35°C with reciprocal shaking, *Cupriavidus* sp. KNK-J915 cells were collected by centrifugation from 4.2 L of the cultured broth (from Sakaguchi flask × 36), washed with 100 mL of 100 mM potassium phosphate (pH 7.0), and suspended in 200 mL of 100 mM potassium phosphate (pH 7.0). All purification procedures were performed at 4°C. After ultrasonic disruption of the cells, using an ultrasonic homogenizer UH-600 S (SMT Co., Ltd., Tokyo, Japan) for 10 min (pulse 50%, output 10, 1 min × 10), 151 mL of cell-free extract were obtained by centrifugation. Ammonium sulfate was added to the cell-free extract to reach a saturation concentration of 20%, and the mixture was stirred for 0.5 h. The precipitate was discarded after centrifugation. In addition, ammonium sulfate was added to the supernatant to reach a saturation concentration of 40%. After being stirred for 0.5 h, the mixture was centrifuged to obtain the formed precipitates, and the precipitates were suspended in 40 mL of 100 mM potassium phosphate (pH 7.0) and dialyzed with 10 mM potassium phosphate (pH 8.0). The dialyzed enzyme solution (67 mL) was applied to a 400-mL Toyopearl DEAE-650 M column (Tosoh, Tokyo, Japan) equilibrated with 10 mM potassium phosphate (pH 8.0). The enzyme was eluted with a 0–0.3 M sodium chloride linear gradient. In total, 200 mL of enzyme solution of the active fractions were collected and dialyzed with 10 mM potassium phosphate (pH 7.0). Ammonium sulfate was added to the dialyzed enzyme solution to give a final concentration of 0.8 M. The enzyme solution (190 mL) was applied to a 75-mL Toyopearl Phenyl-650 M column (Tosoh) equilibrated with 10 mM potassium phosphate (pH 7.0) containing 0.8 M ammonium sulfate. The enzyme was eluted with a 0–0.8 M ammonium sulfate linear gradient. In total, 30 mL of enzyme solution of the active fractions were collected and dialyzed with 10 mM potassium phosphate (pH 7.0). Ammonium sulfate was added to the dialyzed enzyme solution to give a final concentration of 0.8 M. The enzyme solution (26 mL) was applied to a 25-mL Toyopearl Butyl-650S column (Tosoh) equilibrated with 10 mM potassium phosphate (pH 7.0) containing 0.8 M ammonium sulfate. The enzyme was eluted with a 0–0.8 M ammonium sulfate linear gradient. Ten milliliters of the enzyme solution of the active fractions were collected and dialyzed with 10 mM potassium phosphate (pH 8.0). The dialyzed enzyme solution (9.5 mL) was applied to a 6-mL Resource Q column (GE Healthcare Bio-Sciences) equilibrated with 10 mM potassium phosphate (pH 8.0). The enzyme was eluted with a 0–0.5 M sodium chloride linear gradient. In total, 1.9 mL of the enzyme solution of the active

fractions were collected. The active fraction was used as the purified enzyme.

Determination of enzyme molecular weight

The molecular weight of the native enzyme was estimated by column chromatography using a Superdex 200 HR 10/30 column (24 mL; GE Healthcare Bio-Sciences) and standard molecular markers in 50 mM potassium phosphate buffer (pH 7.0) containing 150 mM sodium chloride. The molecular weight of the subunit was estimated by SDS-PAGE (10 %) with SDS-PAGE markers as the standard.

Partial amino acid sequence

CsAM was separated from other peptides by HPLC on a YMC-Pack PROTEIN-RP column (4.6 × 250 mm; YMC) equilibrated with 0.1% trifluoroacetic acid and eluted with a linear acetonitrile gradient (10%–70%) at a flow rate of 1.0 mL/min. The HPLC-purified CsAM was digested with lysyl endopeptidase (Wako Pure Chemicals) in 4 M urea and 50 mM Tris-HCl buffer (pH 9.0) for 24 h at 30°C. Then, the peptides were separated by HPLC as described above. The sequence was analyzed with a model 477A gas-liquid-phase protein sequencer (Applied Biosystems, Carlsbad, CA, USA).

PCR for the core region of the CsAM gene

PCR amplification was performed in a reaction mixture (50 µL) containing 100 ng of chromosomal DNA as a template, both primers (40 pmol each), four dNTPs (final concentration, 10 nmol each), and 2.5 U of Ex Taq DNA polymerase in the buffer for the polymerase. Two oligonucleotide primers, CsAM-F (5'-GAYATHCARACNTTRCARAC-3') and CsAM-C (5'-CCNGCDATRTTRAANAGRTC-3') were synthesized and used. The reaction was performed for 30 cycles (1 min at 95°C, 1 min at 50°C, and 0.5 min at 72°C) using a program temperature control system PC-701 (ASTECC, Fukuoka, Japan). The DNA fragment amplified by PCR was purified and ligated with a pT7Blue T-vector (Merck, Darmstadt, Germany) using a DNA Ligation Kit.

Inverse PCR for DNA sequences flanking the core region

Chromosomal DNA from *Cupriavidus* sp. KNK-J915 was digested with *Pst*I for 18 h

at 37°C. The digested DNA was circularized with T4 DNA ligase. Two oligonucleotide primers, *CsAM-iF* (5'-TGGCAGGCCTGCCGGTTTCGGTCA-3') and *CsAM-iR* (5'-GGAGACCGCGCCATCGTGAAGTCT-3'), were synthesized. Amplification by inverse PCR was performed in reaction mixtures (50 µL) containing 200 ng of circularized DNA obtained as previously described, both primers (50 pmol each), four dNTPs (final concentration, 10 nmol each), and 2.5 U of Ex Taq DNA polymerase in the buffer for the polymerase. The reaction was performed for 30 cycles (1 min at 97°C, 1 min at 60°C, and 5 min at 72°C). The amplified DNA fragment was ligated with a pT7Blue T-vector.

Construction of a *CsAM* expression plasmid

An expression plasmid, pNTCsAM, containing the *CsAM* gene, the lac promoter, and a terminator inserted in pUC19, was constructed. An N-terminus DNA primer (5'-AGCATCGTACATATG-CCTACGGATATCCAGACATTAC-3') having an *NdeI* site added to the initiation codon of the *CsAM* gene and a C-terminus DNA primer (5'-GCAGAATTCTTATCAGGCGGCCGGCTTGACGATGGATT-3') having an *EcoRI* site added immediately after the termination codon were synthesized. The *CsAM* gene was amplified by PCR with the two aforementioned primers from the genomic DNA of *Cupriavidus* sp. KNK-J915. Amplification by PCR was conducted in a reaction mixture (50 µL) containing 10 ng of chromosomal DNA as template, both primers (50 pmol each), four dNTPs (final concentration, 10 nmol each), and 2.5 U of Ex Taq DNA polymerase in the buffer for the polymerase. The reaction was performed for 30 cycles (1 min at 97°C, 1 min at 60°C, and 1.5 min at 72°C). The resulting DNA fragment was digested with *NdeI* and *EcoRI* and then inserted into the *NdeI-EcoRI* sites of pUCNT [16] to obtain the recombinant plasmid pNTCsAM. pNTCsAM was used to transform into *E. coli* HB101.

Construction of a *CnAM* expression plasmid

An expression plasmid, pNTCnAM, containing the *CnAM* (accession no. AAZ60748) gene, the lac promoter, and a terminator inserted in pUC19, was constructed. An N-terminus DNA primer (5'-AGCATCGTACATATGCTTCCTGACCTCAACACACTGC-3') having an *NdeI* site added to the initiation codon of the *CnAM* gene, and a C-terminus DNA primer (5'-GCAGAGCTCCTATTATTC-GTCGCGCAGGGAAGGCTGC-3') having a *SacI*

site added immediately after the termination codon was synthesized. The *CnAM* gene was amplified by PCR with the two aforementioned primers from the genomic DNA of *Cupriavidus necator* JMP134. Amplification by PCR was conducted in a reaction mixture (50 μ L) containing 10 ng of chromosomal DNA as template, both primers (50 pmol each), four dNTPs (final concentration, 10 nmol each), and 2.5 U of Ex Taq DNA polymerase in the buffer for the polymerase. The reaction was performed for 30 cycles (1 min at 98°C, 1 min at 60°C, and 1.5 min at 72°C). The resulting DNA fragment was digested with *NdeI* and *SacI* and then inserted into the *NdeI-SacI* sites of pUCNT [16] to obtain the recombinant plasmid pNTCnAM, which was used to transform into *E. coli* HB101.

General procedure for the chemoenzymatic synthesis of (*R*)-isovaline

CsAM transformed *E. coli* was cultured at 30°C for 10 h in a test tube containing 5 mL of 2-YT medium. The seed culture (1 mL) was then inoculated in a 500-mL Sakaguchi flask containing 50 mL of 2-YT medium. After 20 h incubation at 30°C with reciprocal shaking (130 rpm), the cultured cells were collected by centrifugation from 1.0 L of the cultured broth (from twenty-one Sakaguchi flasks) and were suspended in 1.0 L of water. 2-ethyl-2-methyl-malonamide (EMM) (80 g, 0.55 mol) and the cultured cell suspensions (860 mL) were stirred at 30°C for 22 h. The pH of the reaction mixture was maintained at 7.0 with 30% sodium hydroxide solution. The resulting mixture was centrifuged, and the supernatant was adjusted to pH 12.0 with 30% sodium hydroxide solution. Ammonia in the mixture was removed by evaporation under reduced pressure and concentrated to give the crude mixture (273 g) which contains (*S*)-2-ethyl-2-methyl-malonamic acid (EMA).

A solution of 13% hypochlorous acid (481 g, 0.83 mol), 48% sodium hydroxide solution (138 g, 1.65 mol), crude mixture (273 g) which contains (*S*)-EMA, and water (10 g) were stirred at 0°C for 2 h, and the mixture was heated to 20°C and stirred for 2.5 h. Subsequently, the pH of the mixture was adjusted to 4.0 with concentrated hydrochloric acid (238 g, 2.28 mol) and stirred at 20°C for 25 h to yield crude (*R*)-isovaline hydrochloride. The resulting mixture, sodium hydroxide (23.0 g, 0.56 mol), 2-propanol (169 g), and di-*tert*-butyl dicarbonate (143 g, 0.65 mol) were stirred at 40°C for 3.5 h, and the pH was maintained at 11.0 by the addition of sodium hydroxide (68.5 g, 1.66 mol). The resulting mixture was stirred at 40°C for 2 h and was cooled to 0°C and stirred for 15 h. Concentrated hydrochloric acid

(235 g, 2.26 mol) was added to the resulting mixture and the mixture was heated to 18°C. The organic layer was separated and evaporated under reduced pressure. Toluene (423 g) and water (212 g) were added to the concentrate and the organic layer (560.0 g) was separated and evaporated under reduced pressure to give the crude concentrate containing (*R*)-*N*-Boc-isovaline (118 g, 0.54 mol). Crude (*R*)-*N*-Boc-isovaline was dissolved in dichloromethane (1175 g), and methanesulfonic acid (62.4 g, 0.65 mol) was added. The mixture was stirred at 24°C for 5 h. The resulting mixture was evaporated under reduced pressure to give the crude concentrate containing (*R*)-isovaline mesylate. Crude (*R*)-isovaline mesylate was dissolved in acetone (1175 g), and triethylamine (68.4 g, 0.68 mol) was added. The mixture was stirred at 24°C for 4 h. The solid matter precipitated and was filtered, washed with acetone, and dried to give (*R*)-isovaline (48.7 g, 0.42 mol) as a white solid in 74.9% yield. Characterization of (*R*)-isovaline [36]: ¹H-NMR (500 MHz, D₂O) δ (ppm): 1.74 (m, 1H), 1.59 (m, 1H), 1.30 (s, 3H), 0.75 (t, 3H, *J* = 7.5 Hz). [α]_D²⁵ = -8.2 (c = 1.0, H₂O).

RESULTS

Screening of (*S*)-selective BNPD-hydrolyzing microorganisms

A total of 468 strains were examined for their ability to hydrolyze BNPD to BNPA. Twenty-four strains exhibited (*S*)-selectivity, and 12 strains displayed (*R*)-selectivity. Among the 24 strains that exhibited (*S*)-selectivity, further selection of the most suitable strain was performed. Of those, *Cupriavidus* sp. KNK-J915 was selected as the most promising amidase source with a focus on its activity and stereoselectivity (*E*-value, 185) (Table 3-1). No amide or nitrile compounds enhanced amidase activity in the cells, suggesting constitutive expression of the enzyme.

Table 3-1 Hydrolysis of (*RS*)-BNPD by cells of *Cupriavidus* sp. KNK-J915.

Microorganism	Conversion (%)	Remaining BNPD	
		Stereoselectivity (% <i>e.e.</i>)	<i>E</i> -value
<i>Cupriavidus</i> sp. KNK-J915 FERM BP-10739	52	99.9 (<i>R</i>)	185

Purification of (*S*)-selective BNPD-hydrolyzing enzyme (*CsAM*)

Cupriavidus sp. KNK-J915 was cultured in 4.2 L of medium P, and *CsAM* was purified from the cell-free extract of cultured cells by four-column chromatography. The specific amidase activity for (*RS*)-BNPD (45.8 mM) was 1.67 U/mg (Table 3-2). The purified enzyme catalyzed the hydrolysis of BNPD with (*S*)-stereoselectivity (*E*-value, > 200). The purified enzyme gave a single band with an apparent subunit molecular weight of 47,000 on SDS-PAGE (Fig. 3-3). Gel filtration column chromatography showed that molecular weight of the native *CsAM* was 200,000, indicating that the native *CsAM* was a tetramer.

Table 3-2 Purification of amidase from *Cupriavidus* sp. KNK-J915.

Step	Total protein (mg)	Total activity (mU)	Specific activity (mU/mg)	Yield (%)
Cell-free extract	6040	7127	1	100
Ammonium sulfate	2265	7611	3	107
TOYOPEARL DEAE-650M	1045	5871	6	82
TOYOPEARL Phenyl-650M	6	3224	512	45
TOYOPEARL Butyl-650S	3	1699	655	24
RESOURCE Q	0.3	469	1670	7

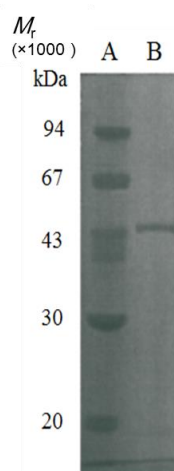


Figure 3-3. SDS-PAGE of the CsAM from *Cupriavidus* sp. KNK-J915. (A) Molecular weight marker proteins: phosphorylase b (94,000), bovine serum albumin (67,000), ovalbumin (43,000), carbonic anhydrase (30,000), trypsin inhibitor (20,000), (B) purified enzyme.

Effects of temperature and pH on the stability and activity of CsAM

The stability of the purified enzyme was examined at various temperatures. After the enzyme had been incubated for 0.5 h at various temperatures, its activity was assayed with (*RS*)-BNPD as a substrate under the standard conditions. The enzyme exhibited the following remaining activity: 60°C, 14.5%; 55°C, 88.2%; 50°C, 99.8%; 45°C, 100%; 40°C, 100%; and 30°C, 100% (Fig. 3-4). The enzyme reaction was performed at various temperatures under standard enzyme assay conditions. The maximum activity for the hydrolysis of (*RS*)-BNPD was at 50°C. At temperatures exceeding 50°C, the activity rapidly decreased because of the instability of the enzyme at higher temperatures (Fig. 3-4).

The stability of the enzyme was also examined at various pH values. The enzyme was incubated at 30°C for 0.5 h in the following buffers (100 mM): citrate/NaOH (pH 4.0–6.0),

potassium phosphate (pH 6.0–8.0), Tris/HCl (pH 8.0–9.0), carbonate (pH 9.0–10), and glycine/NaOH (pH 10–12). Then, a sample of the enzyme solution was taken, and the remaining activity of the purified enzyme was assayed under standard conditions. The enzyme was unstable in the pH range 4.0–6.0. The optimal pH for the activity of the enzyme was measured in the previously described buffers. The enzyme displayed maximum activity at pH 8.0–9.0.

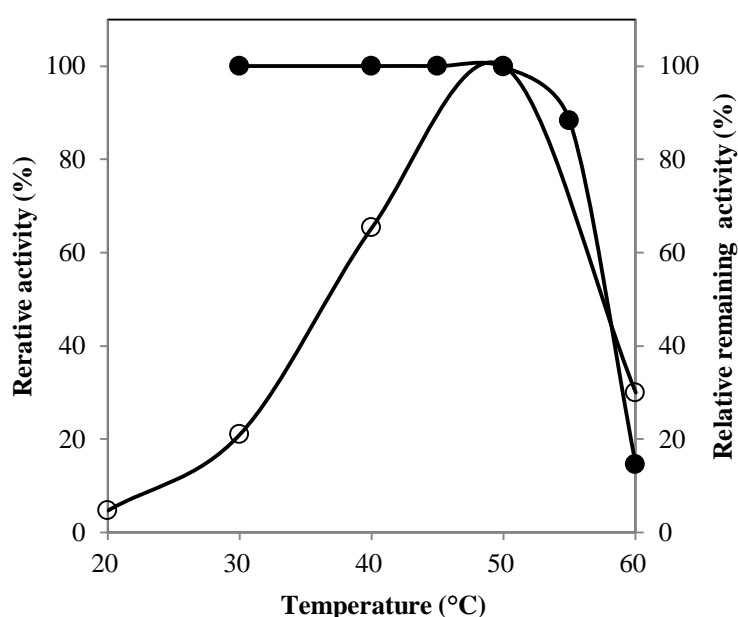
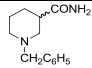
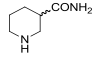
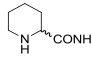
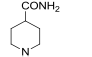
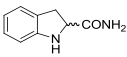
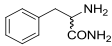
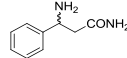
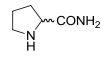
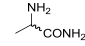
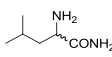
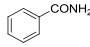
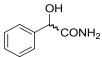
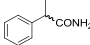


Figure 3-4. Effect of temperature on the activity and stability of the CsAM from *Cupriavidus* sp. KNK-J915. The activity was assayed using 45.8 mM (*RS*)-BNPD. *open circles*, effect of temperature on the activity; and *closed circles*, heat stability.

Substrate specificity

To study the substrate specificity of the enzyme, the purified CsAM was used to hydrolyze various amides, and the activity was assayed (Table 3-3). The enzyme hydrolyzed various nitrogen-containing heterocyclic amides and aliphatic amides excluding acetamide. In contrast, the enzyme could not hydrolyze the following amino acid amides: DL- β -phenylalanine amide, DL-prolinamide, DL-alanine amide, and DL-leucine amide.

Table 3-3 Substrate specificity of the CsAM purified from *Cupriavidus* sp. KNK-J915.

Substrate	Chemical formula	Relative activity (%)
(<i>RS</i>)- <i>N</i> -benzyl-piperidine-3-carboxamide (BNPD)		100
(<i>RS</i>)-piperidine-3-carboxamide (NPD)		203
(<i>RS</i>)-piperidine-2-carboxamide		70
Piperidine-4-carboxamide		43
(<i>RS</i>)-indoline-2-carboxylic acid amide		130
DL-phenylalanine amide		7
DL-β-phenylalanine amide		Not detected
DL-prolinamide		Not detected
DL-alanine amide		Not detected
DL-leucine amide		Not detected
Benzamide		11
Acetamide	CH ₃ CONH ₂	Not detected
Propionamide	CH ₃ CH ₂ CONH ₂	120
Isobutylamide	(CH ₃) ₂ CH-CONH ₂	470
(<i>RS</i>)-mandelic acid amide		100
(<i>RS</i>)-2-phenyl propionic acid amide		630

Partial amino acid sequence of CsAM

CsAM was separated from the other peptides by reversed-phase HPLC, and the N-terminal amino acid sequence was analyzed using a protein sequencer. The sequence was as follows: PTDIQTLQTRLHDGAVSRADVIAQAAQHAQQPDAHAVFLH. Furthermore, the purified CsAM was digested with lysyl endopeptidase to sequence the internal amino acid sequence. One peptide was separated by reversed-phase HPLC, and its amino acid sequence was analyzed. The sequence was as follows: DLFNIAGEASRAGSPVRSDALAATADATVV.

Cloning and nucleotide sequence of the *CsAM* gene

On the basis of the amino acid sequences of the N-terminal peptides and internal peptide, the primers *CsAM-F* and *CsAM-R* were synthesized. The core region of the *CsAM* gene was obtained by PCR using these primers. The PCR product was cloned into the pT7Blue T-vector and sequenced. The core region was 196 bp in length. To clone the 5' - and 3' -flanking regions of the core region, self-circularized DNA of the *Pst*I-digested chromosomal genome was used as the template for inverse PCR. On the basis of the nucleotide sequence of the core region of the *CsAM* gene, the primers *CsAM-iF* and *CsAM-iR* were synthesized. The 5' - and 3' -flanking regions of the core region were obtained by PCR using the primers *CsAM-iF* and *CsAM-iR*. The PCR product was cloned into the pT7Blue T-vector and sequenced. The nucleotide sequences of the 5' - and 3' -flanking regions and core region were connected, and the initiation codon ATG and terminal codon TGA were identified. The *CsAM* gene data were deposited in the DDBJ DNA database under the accession number AB969679. There was one open reading frame (1341 bp, 447 amino acids), and the deduced amino acid sequence was identical to the partial amino acid sequence found by peptide sequencing. The predicted molecular weight of 46,388 was nearly identical to the molecular weight of 47,000, as estimated by SDS-PAGE.

Amino acid sequence of *CsAM*

The deduced amino acid sequence of *CsAM* was compared with other protein sequences using the BLAST search tool. Database analysis revealed that *CsAM* exhibited identity with a putative amidase of *Cupriavidus necator* JMP134 (78%: Accession No. AAZ60758; referred to as *CnAM*; Fig. 3-5), a putative amidase of *Cupriavidus taiwanensis* LMG19424 (76%: Accession No. CAQ69396), and an amidase of *Rhodococcus rhodochrous* J1 (8.5%: Accession No. BAA03744) [37].

CsAM	1	MPTDICTLQTRRHIDGAVSRADVITACAAQHAQQEDAHAVFLHITFDTAQVAKRADAACLAKKPLHPLAGL	70
CnAM	1	MLEDLNLTTHARLREGAISRVELTEAAADAAASQBRACAVFLHSTFDTAIQDARAADAAGRAGKALHPLAGL	70
CsAM	71	PVSVKDLNENIAGEASRAGSPVRSDDALAAATADATVVRRRLRESGAALVGRTNMTEFAFSGVGINPHFGTIPVN	140
CnAM	71	PVSVKDLNEDVAGEVTRAAASAVRHDAPEATADATVVARRLHA GAALVGRTNMTEFAFSGVGINPHFGTIPVN	140
CsAM	141	PADKQ-VARIPGGSSSGAAVSVVALGLAVAGLGSDTGGSIRIPAALCGLTGFKPTARRVPLDGAFPLSYTL	209
CnAM	141	PASADGLARIPGGSSSGAAVSVVALGLAVAGLGSDTGGSIRIPAALCGLTGFKPTARRVPLDGAFPLSYTL	210
CsAM	210	DTACAMARTVQDCVLVDSVIADQAVLPEVIKGAAGIRLAIIPRQVLLDDLDIVARAFDRALGRLSAAGVQI	279
CnAM	211	DTACAMARTVNDCLLVDSVIADNMLVESAPAAALRLAIIPRQVLLDDLDIVARAFDRALGRLSAAGVQL	280
CsAM	280	EHIDLPELAEIATINASGGFTAAEAHATHRHVLATRRQYDPRVASRIDRGAAMSADYVDLARRARIDWI	349
CnAM	281	EHIDLPELAEIPLGNAAGGFSAAEAHATHRHVLATRRMLYDPRVAIRIDRGAAMSADYVDLARRARIDWI	350
CsAM	350	TRVAAARLZGFDAVACPTVPMVAFPIAIPLVADDALFFHTNALLRNTSAFNFLDGGCSISLPCHPDELVPVG	419
CnAM	351	SRVAAARLARFDAVICPTVPMVAFPIEPLRADDLFLRNTNALLRNTSAFNFLDGGCSISLPCHPDELVPVG	420
CsAM	420	LMLSHGATPRDAQLIGTAALESIVKFAA—	447
CnAM	421	LMLSHGATPRDAQLIGTAALESIVQESLRDE	451

Figure 3-5. Comparison of the amino acid sequences of the CsAM and CnAM. Identical amino acids among the sequences are marked in black. CsAM, an amidase of *Cupriavidus* sp. KNK-J915 (Accession No. AB969679), CnAM, a putative amidase of *Cupriavidus necator* JMP134 (78% identity: Accession No. AAZ60758).

Enantioselectivity of CsAM and CnAM for (RS)-BNPD and (RS)-NPD

The plasmids pNTCsAM and pNTCnAM were used to transform into *E. coli* HB101. Using the transformed *E. coli* cells, the stereoselectivities of CsAM and CnAM for (RS)-BNPD and (RS)-NPD were examined and compared. Tables 3-4 and 3-5 present the enantioselectivities of these enzymes in the presence of (RS)-BNPD and (RS)-NPD. CsAM catalyzed the hydrolysis of both (RS)-BNPD and (RS)-NPD with high (*S*)-selectivity (*E*-value, 127 and > 200, respectively). CnAM catalyzed the hydrolysis of (RS)-BNPD with high (*S*)-selectivity (*E*-value, 175). In contrast, it catalyzed the hydrolysis of (RS)-NPD with a very low level of (*S*)-selectivity (*E*-value, 7).

Table 3-4 Stereoselectivity of *CsAM* and *CnAM* for (*RS*)-BNPD.

Amidase	Conversion (%)	Remaining BNPD	
		Stereoselectivity (% <i>e.e.</i>)	<i>E</i> -value
<i>CsAM</i>	52.9	99.9 (<i>R</i>)	127
<i>CnAM</i>	51.5	99.4 (<i>R</i>)	175

Table 3-5 Stereoselectivity of *CsAM* and *CnAM* for (*RS*)-NPD.

Amidase	Conversion (%)	Remaining NPD	
		Stereoselectivity (% <i>e.e.</i>)	<i>E</i> -value
<i>CsAM</i>	50.2	98.3 (<i>R</i>)	> 200
<i>CnAM</i>	30.9	29.9 (<i>R</i>)	7

***CsAM*-catalyzed asymmetric hydrolysis of 2-ethyl-2-methyl-malonamide**

The production of (*S*)-EMA from EMM was investigated using cultured cells of *CsAM*-producing recombinant *E. coli*. The effect of temperature and substrate concentration on the enantioselective hydrolysis of EMM was studied. This enzyme was stable at high temperatures, as reported above, as no decrease in activity was observed even after 30 min at 50°C. As shown in Fig. 3-6, under incubation at 30°C, 208 mM and 624 mM of EMM were consumed after 6 h and 19 h, respectively, and the optical purity of the produced (*S*)-EMA were 99.0% *e.e.* and 98.6% *e.e.*, respectively. Under incubation at 40°C, 208 mM and 624 mM of EMM were consumed after 4 h and 10 h, respectively, and the enantiomeric excesses of the produced (*S*)-EMA were 98.4% *e.e.* and 98.0% *e.e.*, respectively. The reaction speed increased with increasing temperature, from 30°C to 40°C. Higher reaction temperatures and substrate concentrations led to lower enantiomeric excesses of (*S*)-EMA (Table 3-6). The production of ethylmethylmalonic acid was not observed under any conditions, suggesting that *CsAM* does not exert activity on (*S*)-EMA, and (*S*)-EMA is produced nearly quantitatively from EMM. Based on the aforementioned results, 30°C and 624 mM were chosen as the optimal temperature and substrate concentration for subsequent experiments.

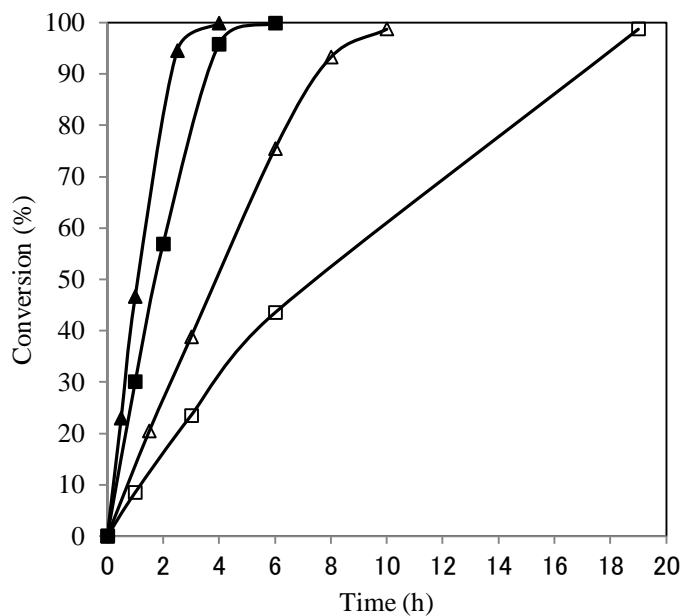


Figure 3-6. Time courses of CsAM-catalyzed asymmetric hydrolysis of EMM.

The reaction mixture consisted of EMM (30 mg, 208 μ mol, or 90 mg, 624 μ mol) and the cell suspensions (1 mL). The bioconversion was carried out at 30°C or 40°C.

Symbols: 40°C 208mM (▲), 30°C 208 mM (■), 40°C 624 mM (△), 30°C 624 mM (□).

Table 3-6 Effects of substrate concentration and temperature on the enantioselectivity of CsAM-catalyzed asymmetric hydrolysis.

EMM Concentration (mM)	Temperature (°C)	Produced (<i>S</i>)-EMA Stereoselectivity (% <i>e.e.</i>)
208	30	99.0
	40	98.4
624	30	98.6
	40	98.0

Chemoenzymatic production of (*R*)-isovaline

Starting from diethyl 2-methylmalonate, a relatively inexpensive raw material, I obtained (*R*)-isovaline in 58.6% yield in eight steps, including the *Cs*AM-catalyzed asymmetric hydrolysis of EMM (Fig. 3-7).

EMM (80 g, 0.55 mol) and the cultured cell suspensions (860 mL) were stirred at 30°C for 22 h. The enantiomeric excess of the produced (*S*)-EMA was 98.6% *e.e.*. Using the (*S*)-EMA solution, the preparation of (*R*)-isovaline (48.7 g, 0.42 mol) could be accomplished, via the Hofmann rearrangement and neutralization crystallization, in 74.9% yield. From acetone-containing crude (*R*)-isovaline mesylate, (*R*)-isovaline was recrystallized by the addition of triethylamine. The enantiomeric excess of (*R*)-isovaline was increased to 99.1% *e.e.* due to the recrystallization. Therefore, the feasibility of a chemoenzymatic, large scale production of (*R*)-isovaline with high enantiomeric excess was confirmed.

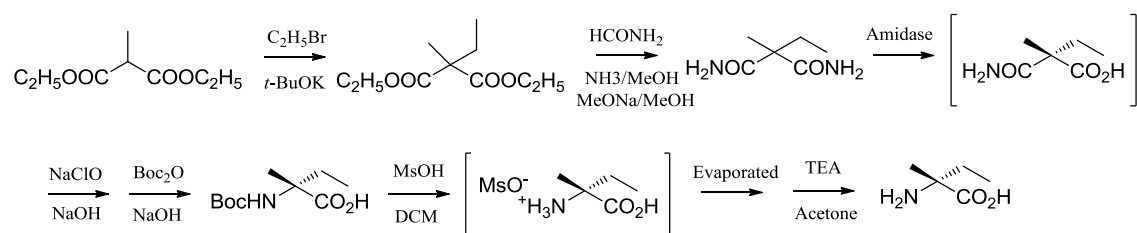


Figure 3-7. Preparative chemoenzymatic production of (*R*)-isovaline.

DISCUSSION

(*R*)-NPD is a useful intermediate for the synthesis of (*R*)-3-aminopiperidine, an optically active amine used as the substructure of certain DPP-4 inhibitors. Because (*RS*)-NPD is a relatively inexpensive raw material, enzymatic stereoselective resolution of the enantiomeric mixture represents an efficient synthetic strategy to prepare (*R*)-NPD. An amidase with high (*S*)-selectivity is required to produce (*R*)-NPD of high optical purity according to this synthetic strategy.

Of the 468 strains screened, *Cupriavidus* sp. KNK-J915 was chosen as the most promising strain because it displayed (*RS*)-NPD-hydrolyzing activity with the highest (*S*)-selectivity. I purified an (*S*)-specific, (*RS*)-NPD-hydrolyzing enzyme from *Cupriavidus* sp. KNK-J915 and verified that the enzyme (*CsAM*) hydrolyzes (*RS*)-NPD in a strictly (*S*)-selective manner (*E*-value, 200). Further, substrate specificity analysis of the purified enzyme indicated that the enzyme exerted hydrolyzing activity on some amides as shown in Table 3-3, particularly various nitrogen-containing heterocyclic amides including (*RS*)-piperidine-2-carboxamide. However, the enzyme was not active against L-prolinamide. (*S*)-selective piperazine-2-tert-butylcaroxamide amidase (*LaaA*) from *Pseudomonas* sp. has been reported to act on both (*RS*)-piperidine-2-carboxamide and L-prolinamide [38]. Therefore, the enzyme purified from *Cupriavidus* sp. KNK-J915 appears to have different characteristics than *LaaA* in terms of substrate recognition.

I determined the amino acid sequence of the purified enzyme, after which I cloned and sequenced the gene encoding the enzyme. A putative amidase from *C. necator* (referred to as *CnAM*) was found to be most similar to *CsAM* in the deduced amino acid sequence, exhibiting 78% identity (Fig. 3-5). Therefore, one can argue that *CsAM* is a novel amidase. I analyzed the stereoselectivity of *CsAM* and *CnAM* in the hydrolysis of (*RS*)-BNPD and (*RS*)-NPD using cultured cells of recombinant *E. coli* producing *CsAM* or *CnAM*. The result illustrated that *CsAM* was highly (*S*)-selective for both (*RS*)-BNPD and (*RS*)-NPD (*E*-values, 127 and > 200, respectively). In contrast, *CnAM* hydrolyzed (*RS*)-NPD but with a very low level of (*S*)-selectivity (*E*-value, 7), whereas it was highly selective for the (*S*)-form in the hydrolysis of (*RS*)-BNPD (*E*-value, 175). It is intriguing that these enzymes displayed marked differences in selectivity depending on the presence or absence of a benzyl group in the substrates. The sequences of the enzyme differ by 94 amino acids and the resulting

conformational differences are presumably responsible for the aforementioned selectivity differences described. These selectivity differences may be expected to be clarified if conformational analysis of *CsAM* and *CnAM* can be performed.

An efficient chemoenzymatic process for the production of (*R*)-isovaline was developed. An amidase derived from *Rhodococcus rhodochrous* NBRC15564 has been reported to hydrolyze EMM in an (*S*)-selective manner, but the enantiomeric excess of the resulting EMA was very low (12% *e.e.*) [39, 40]. An enantioselective hydrolysis of EMM by chemical- or bio-catalyst that can differentiate between the methyl group and ethyl group has not been reported, with the exception of this example. Cultured cells of recombinant *E. coli* producing *CsAM* served as an excellent catalyst in terms of reaction efficiency, stereoselectivity, and the efficient preparation of (*S*)-EMA. The concentration of EMM was optimized at 624 mM (90 g/L), which yielded (*S*)-EMA in 98.6% *e.e.*. Using the (*S*)-EMA solution, the preparative scale production of (*R*)-isovaline with high enantiomeric excess (99.1% *e.e.*) could be easily accomplished by the Hofmann rearrangement, indicating that a stable biocatalytic process that could be applied on the industrial scale was established in this study. To realize an even more efficient production of (*R*)-isovaline, further studies regarding the enzymatic process are needed, including improving the enantioselectivity of *CsAM* toward EMM under higher reaction temperatures and substrate concentrations through optimization of the reaction pH, protein engineering, preparing for the practical immobilized *CsAM*, and evaluation of the stability of the immobilized enzyme on repeated batch reactions.

SUMMARY

A novel amidase (*CsAM*) acting on (*RS*)-*N*-benzyl-3-piperidinecarboxamide was purified from *Cupriavidus* sp. KNK-J915 (FERM BP-10739) and characterized. The enzyme acts on (*RS*)-*N*-benzyl-3-piperidinecarboxamide (*S*)-selectively to yield (*R*)-*N*-benzyl-3-piperidinecarboxamide. Analytical gel filtration column chromatography and SDS-PAGE revealed that the enzyme is a tetramer with a subunit molecular weight of approximately 47,000. It has a broad substrate spectrum against nitrogen-containing heterocyclic amides. Its optimal pH and temperature are 8.0–9.0 and 50°C, respectively. The *CsAM* gene was cloned and sequenced, and it was found to comprise 1341 bp and encode a polypeptide with a molecular weight of 46,388. The deduced amino acid sequence exhibited 78% identity to that of a putative amidase (*CnAM*) from *Cupriavidus necator* JMP134. The cultured cells of recombinant *Escherichia coli* producing *CnAM* could be used for the (*S*)-selective hydrolysis of (*RS*)-*N*-benzyl-3-piperidinecarboxamide but could not be used for the *S*-selective hydrolysis of (*RS*)-3-piperidinecarboxamide because of its very low level of selectivity. In contrast, the cultured cells of recombinant *E. coli* producing *CsAM* could hydrolyze both (*RS*)-*N*-benzyl-3-piperidinecarboxamide and (*RS*)-3-piperidinecarboxamide with high (*S*)-selectivity.

(*R*)-isovaline has potential applications in the drug development field, and therefore, the development of an efficient method for the production of (*R*)-isovaline is desired. In this study, I investigated the asymmetric hydrolysis of 2-ethyl-2-methyl-malonamide to (*S*)-2-ethyl-2-methyl-malonamic acid, a useful synthetic intermediate in the production of (*R*)-isovaline, using *CsAM*. The produced (*S*)-2-ethyl-2-methyl-malonamic acid (98.6% *e.e.*) could easily be converted to (*R*)-isovaline by the Hofmann rearrangement. Starting from diethyl 2-methylmalonate, we obtained (*R*)-isovaline (99.1% *e.e.*) in 58.6% yield in eight steps, including the *CsAM*-catalyzed asymmetric hydrolysis of 2-ethyl-2-methyl-malonamide.

CONCLUSIONS

As stated in the Introduction, methods utilizing amine transaminases are useful for efficient synthesis of chiral amines, which have been reported as key raw materials for the synthesis of medicinal products that recently entered the market. However, depending on the target amine compound, there are instances when carbonyl compounds cannot be used as the raw material. In some cases, although carbonyl compounds can potentially be used as a substrate, according to theoretical synthetic routes, they show poor chemical stability on an industrial scale; in other instances, it is difficult to obtain large quantities of the substance. In such cases, amine transaminases cannot be used. This study aimed to establish efficient amine synthesis techniques, other than those utilizing amine transaminases. Specifically, my synthetic approach effectively combined the enzymatic preparation of chiral amides using prochiral or racemic amides and imide compounds as the raw material, without using carbonyl compounds, and the Hofmann rearrangement using chiral amides as the raw material.

In Chapter I, I demonstrated the successful preparation of (*R*)-3-(4-chlorophenyl) glutaric acid monoamide (CGM), a precursor of the GABA analog arbaclofen, using prochiral 3-(4-chlorophenyl) glutaric acid diamide as the raw material and *Comamonas* sp. KNK3-7-derived amidase as the enzyme. Furthermore, this amidase was improved by protein engineering techniques, and I also succeeded in significantly increasing its reactivity. It is not described in this paper, but I also confirmed that arbaclofen could be obtained from the (*R*)-CGM prepared by this method using the Hofmann rearrangement reaction.

In Chapter II, I demonstrated the successful preparation of (*R*)-CGM with prochiral 3-(4-chlorophenyl) glutarimide (CGI) as the raw ingredient using *Burkholderia phytofirmans* DSM 17436- and *Alcaligenes faecalis* NBRC 13111-derived imidases. To date, there have been no reports of chiral amide synthesis using imidases, and thus I am the first in the world who discovered that imidases are effective biocatalysts for chiral compound synthesis.

In Chapter III, I demonstrated the successful preparation of the (*R*)-3-aminopiperidine precursor (*R*)-3-piperidinecarboxamide (NPD), which is the key raw material for dipeptidyl peptidase-4 (DPP-4) inhibitors. For the reaction, I used racemic (*RS*)-NPD as the raw material and *Cupriavidus* sp. KNK-J915-derived amidase as the enzyme. It is not described in this paper, but I also confirmed that (*R*)-3-aminopiperidine could be

prepared on an industrial scale by isolating (*R*)-NPD and using the Hofmann rearrangement reaction. Furthermore, I also demonstrated the preparation of the (*R*)-isovaline precursor (*S*)-2-ethyl-2-methyl-malonamic acid (EMA) with prochiral 2-ethyl-2-methyl-malonamide (EMM) as the raw material using this amidase. I was also able to prepare (*R*)-isovaline by using (*S*)-EMA in the Hofmann rearrangement reaction.

In conclusion, I efficiently synthesized chiral amides using amidases and imidases and produced chiral amines by the Hofmann rearrangement. Thus, I was able to establish an efficient chemoenzymatic amine synthesis technique.

REFERENCES

1. Bornscheuer, U. T., Huisman, G. W., Kazlauskas, R. J., Lutz, S., Moore, J. C., Robins, K.: Engineering the third wave of biocatalysis. *Nature*, **485**, 185-94 (2012)
2. Savile, C. K., Janey, J. M., Mundorff, E. C., Moore, J. C., Tam, S., Jarvis, W. R., Colbeck, J. C., Krebber, A., Fleitz, F. J., Brands, J., Devine, P. N., Huisman, G.W., Hughes, G. J.: Biocatalytic asymmetric synthesis of chiral amines from ketones applied to sitagliptin manufacture. *Science*, **329**, 305-9 (2010)
3. Velankar, H., Clarke, K. G., Preez, R. D., Cowan, D. A., Burton, S. G.: Developments in nitrile and amide biotransformation processes. *Trends. Biotechnol.*, **28**, 561-9 (2010)
4. Chen, P., Gao, M., Wang, D. X., Zhao, L., Wang, M. X.: Enantioselective biotransformations of racemic and meso pyrrolidine-2, 5-dicarboxamides and their application in organic synthesis. *J. Org. Chem.*, **77**, 4063-72 (2012)
5. Lal, R., Sukbuntherng, J., Tai, E. H., Upadhyay, S., Yao, F., Warren, M. S., Luo, W., Bu, L., Nguyen, S., Zamora, J., Peng, G., Dias, T., Bao, Y., Ludwikow, M., Phan, T., Scheurman, R. A., Yan, H., Gao, M., Wu, Q. Q., Annamalai, T., Raillard, S. P., Koller, K., Gallop, M. A., Cundy, K. C.: Arbaclofen placarbil, a novel *R*-baclofen prodrug: improved absorption, distribution, metabolism, and elimination properties compared with *R*-baclofen. *J. Pharm. Exp. Ther.*, **330**, 911-21 (2009)
6. Feng, J., Zhang, Z., Wallace, M. B., Stafford, J. A., Kaldor, S. W., Kassel, D. B., Navre, M., Shi, L., Skene, R. J., Asakawa, T., Takeuchi, K., Xu, R., Webb, D. R., Gwaltney, S. L.: Discovery of Alogliptin: A potent, selective, bioavailable, and efficacious inhibitor of dipeptidyl peptidase IV. *J. Med. Chem.*, **50**, 2297-300 (2007)
7. Eckhardt, M, Langkopf, E., Mark, M., Tadayyon, M., Thomas, L., Nar, H., Pfrengle, W., Guth, B., Lotz, R., Sieger, P., Fuchs, H., Himmelsbach, F.: 8-(3-(*R*)-Aminopiperidin-1-yl)-7-but-2-ynyl-3-methyl-1-(4-methyl-quinazolin-2-ylmethyl)-3,7-dihydropurine-2,6-dione (BI 1356), a highly potent, selective, long-acting, and orally bioavailable DPP-4 inhibitor for the treatment of type 2 diabetes. *J. Med. Chem.*, **50**, 6450-53 (2007)
8. Cooke, J. E., Mathers, D. A., Puil, E.: *R*-isovaline: a subtype-specific agonist at GABA_B-receptors?. *Neuroscience.*, **201**, 85-95 (2012)

9. **Hampson, D. R., Adusei, D. C., Pacey, L. K.:** The neurochemical basis for the treatment of autism spectrum disorders and Fragile X Syndrome. *Biochem. Pharmacol.*, **81**, 1078-86 (2011)
10. **Felluga, F., Gombac, V., Pitacco, G., Valentin, E.:** A short and convenient chemoenzymatic synthesis of both enantiomers of 3-phenylGABA and 3-(4-chlorophenyl) GABA (Baclofen). *Tetrahedron. Asymmetry.*, **16**, 1341-45 (2005)
11. **Ji, L., Ma, Y., Li, J., Zhang, L., Zhang, L.:** An efficient synthesis of (*R*)- and (*S*)-baclofen via desymmetrization. *Tetrahedron. Lett.*, **50**, 6166-8 (2009)
12. **Caira, M. R., Clauss, R., Nassimbeni, L. R., Scott, J. L., Wildervanck, A. F.:** Optical resolution of baclofen via diastereomeric salt pair formation between 3-(*p*-chlorophenyl) glutaramic acid and (*S*)-(-)- α -phenylethylamine. *J. Chem. Soc. Perkin. Trans.*, **2**, 763-8 (1997)
13. **Chenevert, R., Desjardin, M.:** Chemoenzymatic enantioselective synthesis of baclofen. *Can. J. Chem.*, **72**, 2312-7 (1994)
14. **Hoekstra, M. S., Sobieray, D. M., Schwindt, M. A., Mulhern, T. A., Grote, T. M., Huckabee, B. K., Hendrickson, V. S., Franklin, L. C., Granger, E. J., Karrick, G. L.:** Chemical development of CI-1008, an enantiomerically pure anticonvulsant., *Org. Process Res. Dev.*, **1**, 26-38 (1997)
15. **Wang, M. X., Liu, C. S., Li, J. S.:** Enzymatic desymmetrization of 3-alkyl- and 3-arylglutaronitriles, a simple and convenient approach to optically active 4-amino-3-phenylbutanoic acids., *Tetrahedron. Asymmetry.*, **12** 3367-73 (2002)
16. **Nanba, H., Ikenaka, Y., Yamada, Y., Yajima, K., Takano, M., Takahashi, S.:** Production of thermotolerant *N*-carbamyl-D-amino acid amidohydrolase by recombinant *Escherichia coli*. *J Biosci Bioeng.*, **87**, 149-54 (1999)
17. **Ohtaki, A., Murata, K., Sato, Y., Noguchi, K., Miyatake, H., Dohmae, N., Yamada, K., Yohda, M., Odaka, M.:** Structure and characterization of amidase from *Rhodococcus* sp. N-771: insight into the molecular mechanism of substrate recognition., *Biochim. Biophys. Acta.*, **1804**, 184-92 (2010)
18. **Kobayashi, M., Komeda, H., Nagasawa, T., Yamada, H., Shimizu, S.:** Occurrence of amidases in the industrial microbe *Rhodococcus rhodochrous* J1. *Biosci. Biotech. Biochem.*, **57**, 1949-50 (1993)

19. Kobayashi, M., Komeda, H., Nagasawa, T., Nishiyama, M., Horinouchi, S., Beppu, T., Yamada, H., Shimizu, S.: Amidase coupled with low-molecular-mass nitrile hydratase from *Rhodococcus rhodochrous* J1. *Eur. J. Biochem.*, **217**, 327-336 (1993)
20. Gavagan, J. E., Fager, S. K., Fallon, R. D., Folsom, P. W., Herkes, F. E., Eisenberg, A., Hann, E. C., DiCosimo, R.: Chemoenzymic production of lactams from aliphatic α,ω -dinitriles. *J. Org. chem.*, **63**, 4792-801 (1998)
21. Petrillo, K. L., Wu, S., Hann, E. C., Cooling, F. B., Bassat, A. B., Gavagan, J. E., DiCosimo, R., Payne, M. S.: Over-expression in *Escherichia coli* of a thermally stable and region-selective nitrile hydratase from *Comamonas testosteroni* 5-MGAM-4D. *Appl. Microbiol. Biotechnol.*, **67**, 664-70 (2005)
22. Hayashi, T., Yamamoto, K., Matsuo, A., Otsubo, K., Muramatsu, S., Matsuda, A., Komatsu, K.: Characterization and cloning of an enantioselective amidase from *Comamonas acidovorans* KPO-2771-4. *J. Ferment. Bioeng.*, **83**, 139-45 (1997)
23. Nagasawa, T., Ryuno, K., Yamada, H.: Superiority of *Pseudomonas chlororaphis* B23 nitrile hydratase as a catalyst for the enzymatic production of acrylamide. *Experientia.*, **45**, 1066-70 (1989)
24. Ciskanik, L. M., Wilczek, J. M., Fallon, R. D.: Purification and characterization of an enantioselective amidase from *Pseudomonas chlororaphis* B23. *Appl. Environ. Microbiol.*, **61** 998-1003 (1995)
25. Pal, D., Chakrabarti, P.: Non-hydrogen bond interactions involving the methionine sulfur atom. *Biomol. Struct. Dyn.*, **19**, 115-28 (2001)
26. Ogawa, J., Soong, C. L., Honda, M., Shimizu, S.: Novel metabolic transformation pathway for cyclic imides in *Blastobacter* sp. Strain A17p-4. *Appl. Environ. Microbiol.*, **62**, 3814-7 (1996)
27. Ogawa, J., Soong, C. L., Honda, M., Shimizu, S.: Imidase, a dihydropyrimidinase-like enzyme involved in the metabolism of cyclic imides. *Eur. J. Biochem.*, **243**, 322-7 (1997)
28. Chavan, A. B., Maikap, G. C., Gurjar, M. K.: An efficient process of racemization of 3-(carbamoylmethyl)-5-methylhexanoic acid: a pregabalin intermediate. *Org. Process. Res. Dev.*, **13**, 812-4 (2009)
29. Ogawa, J., Soong, C. L., Ito, M., Sagawa, T., Prana, T., Prana, M. S., Shimizu, S.: 3-carbamoyl- α -picolinic acid production by imidasecatalyzed regioselective hydrolysis

- of 2,3-pyridinedicarboximide in a water-organic solvent, two-phase system. *Appl. Microbiol. Biotechnol.*, **54**, 331-4 (2000)
30. **Soong, C. L., Ogawa, J., Shimizu, S.**: Cyclic ureide and imide metabolism in microorganisms producing a d-hydantoinase useful for damino acid production. *J. Mol. Catal. B Enzym.*, **12**, 61-70 (2001)
31. **Scott, B. M., Robert, P. H.**: Metal ion dependence of recombinant *Escherichia coli* allantoinase. *J. Bacteriol.*, **185**, 126-34 (2003)
32. **Ramazina, I., Cendron, L., Folli, C., Berni, R., Monteverdi, D., Zanotti, G., Percudani, R.**: Logical identification of an allantoinase analog (puuE) recruited from polysaccharide deacetylases. *J. Biol. Chem.*, **283**, 23295-304 (2008)
33. **Komeda, H., Harada, H., Washika, S., Sakamoto, T., Ueda, M., Asano, Y.**: A novel *R*-stereoselective amidase from *Pseudomonas* sp. MCI3434 acting on piperazine-2-tert-butylcarboxamide. *Eur. J. Biochem.*, **271**, 1580-90 (2004)
34. **Cooke, J. E., Mathers, D. A., Puil, E.**: *R*-Isovaline: a subtype-specific agonist at GABA(B)-receptors?. *Neuroscience*, **201**, 85-95 (2012)
35. **Straathof, A. J. J., Jongejan, J. A.**: The enantiomeric ratio: origin, determination and prediction. *Enzyme Microbiol. Technol.*, **21**, 559-71 (1997)
36. **Green, J. E., Bender, D. M., Jackson, S., O'Donnell, M. J., McCarthy, J. R.**: Mitsunobu approach to the synthesis of optically active α,α -disubstituted amino acids. *Org. Lett.*, **11**, 807-10 (2009)
37. **Kobayashi, M., Komeda, H., Nagasawa, T., Nishiyama, M., Horinouchi, S., Beppu, T., Yamada, H., Shimizu, S.**: Amidase coupled with low-molecular-mass nitrile hydratase from *Rhodococcus rhodochrous* J1. *Eur. J. Biochem.*, **217**, 327-36 (1993)
38. **Komeda, H., Harada, H., Washika, S., Sakamoto, T., Ueda, M., Asano, Y.**: *S*-Stereoselective piperazine-2-tert-butylcarboxamide hydrolase from *Pseudomonas azotoformans* IAM 1603 is a novel L-amino acid amidase. *Eur. J. Biochem.*, **271**, 1465-75 (2004)
39. **Yokoyama, M., Kashiwagi, M., Iwasaki, M., Fukushima, K., Ohta, H., Sugai, T.**: Realization of the synthesis of α,α -disubstituted carbamylacetates and cyanoacetates by either enzymatic or chemical functional group transformation, depending upon the substrate specificity of *Rhodococcus* amidase. *Tetrahedron. Asymmetry.*, **15**, 2817-20 (2004)

40. **Yokoyama, M., Sugai, T., Ohta, H.:** Asymmetric hydrolysis of a disubstituted malononitrile by the aid of a microorganism. *Tetrahedron. Asymmetry.*, **4**, 1081-4 (1993)

ACKNOWLEDGEMENTS

The present thesis is based on the studies carried out from 2005 to 2014 at Kaneka Co. Ltd, and at Laboratory of Fermentation Physiology and Applied Microbiology, Division of Applied Life Sciences, Graduate School of Agriculture, Kyoto University.

I wish to express my sincere thanks to Professor Jun Ogawa of Kyoto University, for his kind guidance, warm understanding and encouragement throughout this study.

I greatly thank Assistant Professor Makoto Hibi for his kindly instruction in experimental technologies, direction of this study, critical reading of the manuscripts, and continuous encouragements.

I am also grateful to Emeritus Professor Sakayu Shimizu for his warm supports, encouragements, and thoughtful advice during the course of this study.

I greatly appreciate to all members of Laboratory of Fermentation Physiology and Applied Microbiology, Division of Applied Life Sciences, Graduate School of Agriculture, Kyoto University; Industrial Microbiology, Graduate School of Agriculture, Kyoto University; Biotechnology Development Laboratories, Kaneka Co. Ltd.

Finally, but not the least, I would like to acknowledge the strong support and affectionate encouragement of my family throughout this study.

PUBLICATIONS

Nojiri, M., Uekita, K., Ohnuki, M., Taoka, N., Yasohara, Y.: Microbial asymmetric hydrolysis of 3-substituted glutaric acid diamides. *J. Appl. Microbiol.*, **115**, 1127-33 (2013)

Nojiri, M., Taoka, N., Yasohara, Y.: Characterization of an enantioselective amidase from *Cupriavidus* sp.KNK-J915 (FERM BP-10739) useful for enzymatic resolution of racemic 3-piperidinecarboxamide. *J. Mol. Catal. B. Enzym.*, **109**, 136-42 (2014)

Nojiri, M., Yoshida, F., Hirai, Y., Nishiyama, A., Yasohara, Y.: A practical chemoenzymatic synthesis of (*R*)-isovaline based on the asymmetric hydrolysis of 2-ethyl-2-methyl-malonamide. *Tetrahedron. Asymmetry.*, **26**, 1-5 (2015)

Nojiri, M., Hibi, M., Shizawa, H., Horinouchi, N., Yasohara, Y., Takahashi, S., Ogawa, J.: Imidase catalyzing desymmetric imide hydrolysis forming optically active 3-substituted glutaric acid monoamides for the synthesis of gamma-aminobutyric acid (GABA) analogs. *Appl. Microbiol. Biotechnol.*, **99**, 9961-9 (2015)

Nojiri, M., Yoshida, S., Kanamaru, H., Yasohara, Y.: Improved efficiency of asymmetric hydrolysis of 3-substituted glutaric acid diamides with an engineered amidase. *J. Appl. Microbiol.*, **120**, 1542-51 (2016)